

NASA Contractor Report 3668

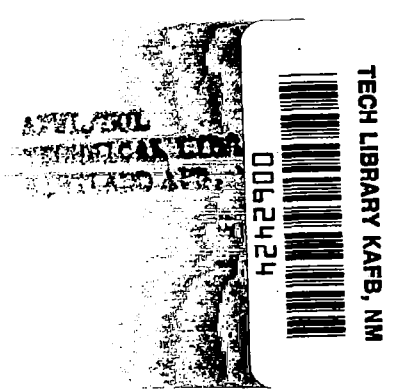
NASA
CR
3668
c.1

ADAM - An Axisymmetric Duct Aeroacoustic Modeling System

A. Louis Abrahamson

JANUARY 1983

NASA





NASA Contractor Report 3668

ADAM - An Axisymmetric Duct Aeroacoustic Modeling System

A. Louis Abrahamson
COMTEK
Grafton, Virginia

Prepared for
Langley Research Center

NASA

National Aeronautics
and Space Administration

**Scientific and Technical
Information Branch**

1983

SUMMARY

ADAM is an acronym for Axisymmetric Duct Aeroacoustic Modeling and is the name of an interconnected system of computer programs for analysing the propagation and attenuation of sound in aeroengine ducts containing realistic compressible subsonic mean flows. It has been developed primarily for research directed towards the reduction of noise emitted from turbofan aircraft engines and includes as two basic components, a streamtube curvature program for determination of the mean flow and a finite element code for solution of the acoustic propagation problem.

The system, which has been specifically tailored for ease of use, is presently installed at NASA Langley Research Center on a Control Data Cyber 175 Computer under the NOS Operating System employing a Tektronix terminal for interactive graphics.

This report describes the scope and organization of the ADAM System and includes a users guide, examples of input data and results for selected cases.

TABLE OF CONTENTS

	<u>Page</u>
1 INTRODUCTION.	1
Background	1
Statement of the Problem	1
Previous Work.	2
Synopsis	3
2 SYSTEM OVERVIEW	5
3 THE COMPRESSIBLE FLOW PROGRAM	9
General.	9
The Streamtube Curvature Method.	9
The Turbulent Boundary Layer Procedure	11
Outline of Program Steps	12
4 THE DUCT ACOUSTICS FINITE ELEMENT PROGRAM	14
Introduction	14
Description of the Mathematical Model.	14
Derivation of Equations.	14
Solution Strategy.	16
Element Derivation	19
Global Matrix Assembly and Boundary Conditions	24
Program Structure.	25
Overview	25
Memory Management and Input Data Structure	25
Recovery and Interpolation of Aerodynamic Data	26
Preparation of Output File	26
Structure of the Finite Element Code	26
5 INTERACTIVE GRAPHICS PROGRAMS	30
Introduction	30
Flow Graphics Program.	30
Acoustic Graphics Program.	30
6 USERS' GUIDE.	33
Comments on ADAM/NOS Interface	33
Running of the GE-STC Program.	33
Operation Under CDC-NOS.	33
Preliminary Comments on Input Data	35
Input Data for the GE-STC Program.	35
Interpretation of Program Output	39
Using the Flow Graphics Program.	41
Operation Under NOS.	41
Notes for an Interactive Session	42

TABLE OF CONTENTS (Continued)

	<u>Page</u>
Running the Acoustic Finite Element Program.	42
Operation Under CDC-NOS.	42
Preparation of the User-Function File.	43
Using the Acoustic Graphics Program.	48
Operation Under NOS.	49
Guide to a Typical Interactive Session	49
 7 EXAMPLES AND DISCUSSION	 52
Model Configuration.	52
Approximate Energy Analysis.	52
STC Analyses	54
Correlation of Approximate Energy Analysis With	
Results of AFE Analyses.	54
Correlation for No Flow.	55
Correlation with Flow.	55
Checkerboarding.	56
 8 SUMMARY	 70

LIST OF FIGURES

<u>Figure</u>	<u>Title</u>	<u>Page</u>
2.1	Simplified Functional Diagram of an ADAM Modeling Sequence.	6
3.1	STC Solution Technique.	11
3.2	Subdivision of Flow Field into Regions and Channels	13
4.1	Rectangular Discretization in a Plane	17
4.2	Matrix Map of the 2-D Rectangular Discretization of Figure 4.1	18
4.3	Rectangular Four-Noded Finite Element	19
4.4	Functional Diagram for Numerical Integration of Finite Element Equations.	28
4.5	Description of Block Tridiagonal Matrix Solution with Memory Map	29
6.1	ADAM System Functional Diagram.	34
6.2	Illustration of a Multiple Channel Configuration.	38

LIST OF FIGURES (Continued)

<u>Figure</u>	<u>Title</u>	<u>Page</u>
6.3	Nonuniform Axial Points Distribution Function for Duct with Central Constriction.	46
7.1	Test Case Geometry: Duct With Central Constriction	52
7.2	Streamlines for Case 2.	58
7.3	Mach Number Contours from .13 to .3 (interval=.01) for Case 2.	58
7.4	Velocity Contours from 42 to 98 (interval=7) for Case 2.	58
7.5	Streamlines for Case 3.	59
7.6	Mach Number Contours from .24 to .68 (interval=.04) for Case 3.	59
7.7	Velocity Contours from 80 to 230 (interval=10) for Case 3.	59
7.8	Axial Plot of Pressure Amplitude for Case 1 (No Flow) . . .	60
7.9	Axial Plot of Pressure Phase for Case 1 (No Flow)	60
7.10	Axial Plot of Axial Velocity Amplitude for Case 1 (No Flow)	61
7.11	Axial Plot of Radial Velocity Amplitude for Case 1 (No Flow)	61
7.12	Axial Plot of Acoustic Flux Integrated over Successive Radial Planes for Case 1 (No Flow)	62
7.13	Radial Plot of Pressure Amplitude for Case 1 (No Flow), Axial Index 50, z = .3763m.	62
7.14	Radial Plot of Pressure Phase for Case 1 (No Flow), Axial Index 50, z = .3763m	62
7.15	Axial Plot of the Real Part of Outer Wall Specific Acoustic Admittance for Case 1 (No Flow).	63
7.16	Axial Plot of the Imaginary Part of Outer Wall Specific Acoustic Admittance for Case 1 (No Flow)	63
7.17	Axial Plot of Pressure Amplitude for Case 2 Flow.	64

LIST OF FIGURES (Continued)

<u>Figure</u>	<u>Title</u>	<u>Page</u>
7.18	Axial Plot of Pressure Phase for Case 2 Flow.	64
7.19	Axial Plot of Axial Velocity Amplitude for Case 2 Flow.	65
7.20	Axial Plot of Acoustic Flux Integrated over Successive Radial Planes for Case 2 Flow	65
7.21	Axial Plot of Pressure Amplitude for Case 3 Flow.	66
7.22	Axial Plot of Pressure Phase for Case 3 Flow.	66
7.23	Axial Plot of Axial Velocity Amplitude for Case 3 Flow.	67
7.24	Axial Plot of Acoustic Flux Integrated over Successive Radial Planes for Case 3 Flow	67
7.25	Axial Plot of Axial Velocity Amplitude for Case 3 Flow.	68
7.26	Axial Plot of Radial Velocity Amplitude for Case 3 Flow.	68
7.27	Radial Plot of Pressure Amplitude for Case 1 (No Flow)	69
REFERENCES	71
Appendix 1 - Input Data Sheets and Specimen Case for GE-STC Program.		74
- Addendum - Additional STC Program Controls.		80
Appendix 2 - Format of AFE12 Output File		82

1 INTRODUCTION

BACKGROUND

ADAM, which is an acronym for Axisymmetric Duct Aeroacoustic Modeling, has its origins in research work on computational duct acoustics sponsored by NASA-Langley Research Center since the mid-1970's. This work had as its goal the achievement of a better understanding of the physics of sound propagation and attenuation in lined aeroengine ducts containing near sonic compressible mean flows.

In performance of this work, tools have been developed as research vehicles both for ad hoc use in particular projects, and also with the impetus to advance computational algorithms to their limits.

From this perspective, the ADAM system should be viewed as a byproduct of research in aeroengine duct acoustics rather than as the result of a predetermined research or development objective. In this context, the system described in this report is an existing capability whose maintenance and development is dependent upon Langley's future orientation and goals in duct acoustics.

STATEMENT OF THE PROBLEM

Mathematically, the linearized, inviscid, duct acoustics problem is usually formulated as a boundary value problem in quantities representing small perturbations of the basic conservation of momentum, energy and continuity equations of fluid dynamics. Two distinct sets of equations result from the perturbation process and these are considered to represent two distinct phenomena within the physical system:

- the unperturbed mean aerodynamic flow field, which is itself unaffected by the presence of acoustic energy propagating through it and
- the acoustic field whose total energy content is unaffected by the mean flow but whose local energy propagation characteristics are affected (sometimes dramatically) by it.

This assumption is only one of many simplifications and generalizations inherent in the process of creating a general purpose computer code to model a class of physical problems. Such assumptions, which lie not only in the realm of physics but also in mathematics and computer science, are sometimes theoretically justifiable, but ultimately rely on careful comparisons with laboratory work for their verification.

In the absence of flow, combined research in computational and experimental duct acoustics has already been instrumental in verifying the theoretical formulation of acoustic boundary conditions^{1,2} and variable geometry effects³.

Now, with the evolution of a model such as ADAM, basic comparisons between experiment and theory regarding the effects of flow on sound propagation and attenuation in ducts can be performed.

PREVIOUS WORK

Computational Acoustics, that is the discipline of obtaining numerical solutions to the partial differential equations of acoustics, had its beginning in the 1970's and is expected to come of age in the 1980's.

Linear duct acoustics has been a leading research area in the development of this methodology. Baumeister^{4,5} presented successive state-of-the-art reviews on numerical techniques in linear duct acoustics citing 86 references in his November 1981 paper⁵. This single statistic indicates the substantial compendium of literature which has accumulated in this field.

Four distinct techniques from the work conducted to date may currently be viewed as contenders for the title of "Most Favored Method in Linear Duct Acoustics":

- Steady state finite element
- Steady state finite difference
- Transient finite difference, and
- Wave envelope method.

Steady state finite element methods, so called because they rely on a spectral decomposition in time, are presently the best developed of these techniques. The finite element method offers the advantage of easily coping with complex geometries and when combined with a direct matrix solution algorithm yields reliable robust computer codes. The principal disadvantage of the method is the substantial computational cost for large problems.

Steady state finite difference methods suffer from the disadvantage of requiring involved geometry mapping while still consuming computational resources comparable to steady state finite element methods. For simple geometries, however, the implementation in computer code is simpler than for steady state finite elements.

Transient finite difference techniques have been developed by Baumeister^{6,7,8} with the motivation of reducing computational requirements relative to steady state methods. A brief note of explanation regarding the importance of computational requirements in evaluating different techniques is necessary. All methods referred to above (including wave envelope techniques) require substantial computer resources for realistic problems. Because of this fact, the magnitude of the differences in computer cost between techniques is highly significant, either for reduced cost, or added capability at comparable cost. Iterative solution of sparse matrices where possible is usually faster than direct solution. Steady state methods are not amendable to iterative solution algorithms because they usually give rise to nonpositive definite or ill-conditioned matrices⁹.

The transient finite difference method, however, is a special case which is amenable to iterative solution and holds the potential for future advances in the state-of-the-art. It does have the disadvantage however of requiring the same involved geometry mapping as the steady state finite difference method and requires further research before it can be regarded as robust, even in simple problems.

Wave envelope methods also base their appeal on reduced computing cost but through a very different precept. Although several different wave envelope implementations exist, they all attempt to utilize the physical reality that while the basic acoustic variables vary rapidly in space in wavelike patterns, their amplitudes do not. Thus, formulations based on amplitudes may be performed on a much coarser grid than formulations based on the variables themselves. Examples of wave envelope formulations are contained in references 10 through 13. Generally these methods continue to hold considerable appeal for solution of acoustic problems.

SYNOPSIS

Principally because of its generality, advanced state of development, and overall robustness, the acoustic analysis implemented in ADAM is a steady state finite element method. This algorithm was originally developed with isoparametric linear elements¹⁴⁻¹⁶ and has been modified to include the optional use of subparametric Hermite elements.

The flow model used in ADAM is the Streamtube Curvature Program¹⁷ developed by the General Electric Company. It is a well tested and thoroughly documented program designed specifically for numerical computations of compressible flow about and within aeroengine nacelles. Its operation is based on the Streamtube Curvature Relaxation Technique¹⁸ and employs the concept of summing a number of pseudo one-dimensional confluent streamtubes to obtain the total flow. To append viscous boundary layer effects onto the inviscid model, an iteration is performed to match a separate boundary layer calculation over each surface with the overall streamtube solution¹⁹.

User interface with both codes has been simplified and the connection between streamtube curvature flow program and acoustic finite element program has been completely automated. Interactive graphics for aerodynamic and acoustic results complete the system.

Since ADAM has evolved from research activity in a young active research field, the techniques implemented within it, while considered the best currently available, are expected to become dated with time. Nevertheless, it is anticipated that the existence of ADAM will be by itself a stimulus to further work and an aid to the verification of new techniques.

Section 2 of this document contains an overview of the system and describes its general organization. It also forms an introduction to the users guide contained in Section 6. Sections 3, 4, and 5 describe the basic components of the system namely, the program to determine the mean flow, the acoustic finite

element code, and the programs for interactive graphics. Sections 7 and 8 contain examples and some comments on the current status of verification and testing.

2 SYSTEM OVERVIEW

The ADAM system consists of five FORTRAN computer programs interconnected through a defined set of data files. It is presently installed at NASA-Langley Research Center on a Control Data Cyber 175 computer under the NOS operating system. User interface with ADAM has been strongly oriented towards Tektronix interactive terminals.

All FORTRAN code has been specifically designed to be reasonably hardware independent. Major hardware dependence is through the "Tektronix Plot 10" graphics system, but this is not considered a major barrier to portability since several other terminals emulate the Tektronix.

The description of the system contained in this report, however, is limited to its installation at NASA-Langley and portability is not guaranteed.

With the aid of the simplified functional diagram contained in Figure 2.1, consider a step-by-step walkthrough of a typical modeling sequence.

Phase A: Determination of Mean Flow

- (1) Preparation of the input file for the General Electric Streamtube Curvature Program.

Principal items to be specified are:

- o Free stream Mach number, ambient pressure, temperature, and fluid properties.
 - o Parameters to control automatic refinement of spatial computational grid.
 - o Duct geometry.
- (2) Execution of GE-STC Program.

The STC program computes the subsonic and transonic field of inviscid compressible flow about and/or within the given geometry. An optional boundary layer analysis evaluates the friction losses and displacement of the inviscid flow. Since the computational mesh does not extend into the boundary layer, its surfaces are displaced by the computed boundary layer thickness. A one-seventh power law Mach number profile is assumed within the boundary layer.

Within limits prescribed by the user, the program computes its own computational grid. Ambient pressure, temperature, and fluid properties, as well as duct geometry and program output in the form of mean flow parameters at nodes of the computational mesh, and are written to an output data file.

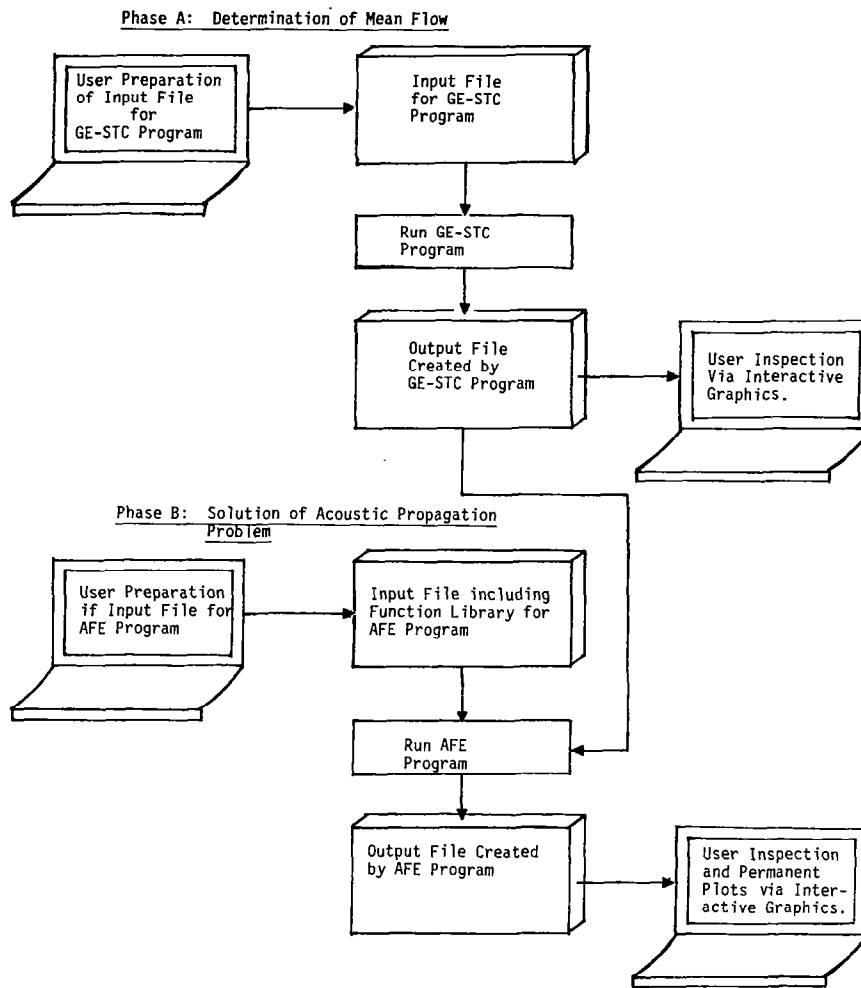


Figure 2.1 Simplified Functional Diagram of an ADAM Modeling Sequence

The user may view streamlines, Mach number contours, or velocity contours plotted over localized sections or over the entire analysis area, and may obtain hard copies of these plots for a permanent record.

Phase B: Solution of the Acoustic Propagation Problem

- (1) User preparation of the input file for Acoustic Finite Element Program.

The acoustic finite element program has been arranged to give the user maximum flexibility for problem specification while at the same time minimizing the quantity of input data required. This has been implemented by allowing the user to specify input in the form of FORTRAN functions.

Principal input parameters are as follows:

- Number of finite elements in r and z directions
- Location of duct section for acoustic analysis within aerodynamic coordinate reference frame
- Frequency and spinning mode number
- Type of finite element to be used in the analysis (linear or Hermite)

Input functions which may be constants, data tables, or analytical functions, include the following:

- Axial and radial grid point distributions
- Inner and outer wall acoustic admittance
- Termination admittance
- Source-plane pressure distribution.

(2) Execution of AFE Program.

The AFE program obtains duct geometry from the GE-STC program output file and creates the mesh for the acoustic finite element analysis. It then obtains the parameters defining the mean aerodynamic flow on the GE-STC mesh and interpolates within this mesh to define the flow field on the acoustic mesh.

Utilizing Hermite or linear finite elements as defined by input data, the program assembles the global finite element matrix by numerically integrating over each finite element and applying boundary conditions as specified in user input admittance and source functions.

A block tridiagonal solver is then applied to obtain primitive acoustic variables consisting of pressure and three components of velocity. Acoustic intensity is integrated over a radial plane at each axial station to give net acoustic flux. All the above results are written to a program output data file.

(3) User Inspection of Results via Interactive Graphics.

Due to the large number of complex nodal variables and the corres-

pondingly greater number of possible interpolation points, some form of graphics is essential for proper user inspection of results.

The interactive graphics program for interrogating the output data has been specially developed for this purpose with the capability not only of displaying stored output data, but also of interpolating within Hermite (or linear) elements or computing special functions such as admittance along a boundary.

The user may request plots of amplitude or phase of any analysis variable along any axial or radial nodal line, specifying optional plot scales. Hard copies of these plots may also be obtained for a permanent record.

3 THE COMPRESSIBLE FLOW PROGRAM

GENERAL

The Streamtube Curvature Analysis (STC) method and its implementation as a computer program for the analysis of aeroengine nacelle flow field properties and drag, is fully described in reference 17. This original program has been slightly modified to produce an output file for use by the Acoustic Finite Element (AFE) program.

A brief summary of the STC theory and computer program structure, together with user instructions are included in this report for completeness. For details not included here, the reader is referred to the original publication.

The STC method solves the inviscid equations of motion over a two-dimensional body (plane or axisymmetric) at transonic speeds. The boundary layer procedure of Stratford and Beavers (SAB) (reference 19) is incorporated to permit evaluation of boundary layer displacement effects and friction drag.

The program may be used to compute both internal flow through the engine nacelle in a number of flow channels as well as external flow around the nacelle. This capability is important for producing accurate flow and drag computations. The acoustic finite element program is currently limited, however, to a single axisymmetric or planar section so that a two-stage analysis as described in Section 6 is necessary for real engines.

Although the program has the capacity to define and iteratively improve its computational mesh, the user has control over the amount of refinement and total mesh size. Geometry is specified in the form of a coordinate list with optional derivatives. Boundary layer effects may be selectively included for any surface and imposed at any level of grid refinement.

THE STREAMTUBE CURVATURE METHOD

The STC program is designed to solve the equations of motion along streamlines ($\Psi = \text{constant}$ lines) and along lines which are orthogonal to the streamlines ($\zeta = \text{constant}$ lines). The variable ζ is introduced to avoid confusion with the velocity potential ϕ which is only applicable when the flow is irrotational.

Across the streamlines, the continuity and Crocco form of the momentum equation are written:

$$\text{Continuity:} \quad \rho A = \frac{\partial \Psi}{\rho |\vec{V}|} \quad (\zeta = \text{Const.}) \quad (3.1)$$

$$\text{Momentum} \quad \frac{1}{2} \frac{\partial (\vec{V}^2)}{\partial n} = -C\vec{V}^2 + \frac{\partial H}{\partial n} - T \frac{\partial S}{\partial n} \quad (\zeta = \text{Const.}) \quad (3.2)$$

Along the streamlines the following forms of the energy and momentum equations apply:

$$\text{Momentum:} \quad \frac{DS}{Ds} = 0 \quad (\psi = \text{Const.}) \quad (3.3)$$

$$\text{Energy} \quad \frac{DH}{Ds} = 0 \quad (\psi = \text{Const.}) \quad (3.4)$$

where

A = Flow cross-sectional area in a streamtube

C = Curvature of the streamline

H = Stagnation enthalpy

n = Distance along the orthogonal

r = Radial coordinate

S = Entropy

s = Distance along the streamline

T = Static temperature

\vec{V} = Velocity

ψ = Stream function

ρ = Density

The solution method is an extension of the conventional streamline curvature method. It is briefly described as follows: First a crude grid of streamlines and orthogonal lines is assumed (see Figure 3.1). Second, the curvature of the streamlines at each of the grid points is evaluated. Third, the momentum equation is integrated along a line normal to the streamlines to obtain velocity, and the continuity equation is integrated to determine the "correct" streamline positions (for the assumed streamline curvature field). These are indicated by the "x" in Figure 3.1. Fourth, an adjustment δn , is computed by considering: (1) the difference between the computed and assumed streamline positions, and (2) the effect of the implied curvature modification in the integrated momentum equation. Finally, the streamlines are repositioned by the δn values.

Because the movement of any one grid point alters, through a change in curvature, the velocity at nearby points, it is desirable to account for these interrelating point adjustments simultaneously. The use of the simultaneous solution procedure employed in the STC program is not part of the classical streamline curvature method. In concept, the set of simultaneous equations for the normal streamline adjustments are formulated from the finite difference equivalent of the following equations:

$$\frac{\partial^2(\delta n)}{\partial \psi^2} + \frac{(1-M^2)}{(\rho V)^2} \frac{\partial^2(\delta n)}{\partial s^2} = F \quad (3.5)$$

where

- δn = Required streamline adjustment in the normal direction
- M = Mach number
- F = Driving (or error) function derived from the solution to the integral continuity and normal momentum equations.

This equation is derived in Ref. 18 for the special case of isentropic two-dimensional flow.

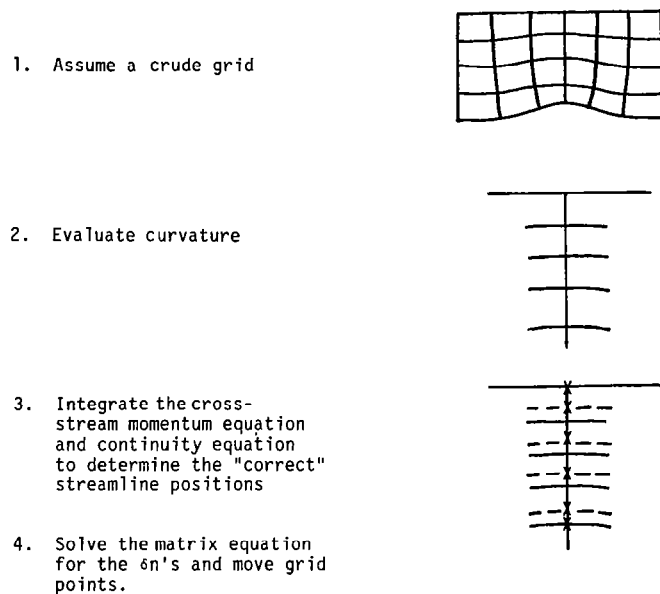


Figure 3.1 STC Solution Technique

THE TURBULENT BOUNDARY LAYER PROCEDURE

The boundary layer procedure which has been coupled with the STC inviscid solution is the method of Stratford and Beavers (SAB) which is described in detail in reference 19. In the SAB method, the integral boundary layer parameters, momentum thickness, displacement thickness, and boundary layer thickness are expressed in closed form as a function of Mach number, equivalent flat plate length, and Reynolds number based on equivalent flat plate length.

Equivalent flat plate length is defined as the length over which a boundary layer growing on a flat plate at the given Mach number would acquire the same thickness as the real boundary layer at that given location.

For axisymmetric or plane flow, this equivalent flat plate length is also defined in closed form as a function of Mach number and distance along the wall (with a radial coordinate in the axisymmetric case).

Boundary layer separation is detected during the calculation by values of the Stratford separation parameter in excess of 0.5.

On a single pass through the STC program, boundary layers are calculated (if required) at the end of the STC process, from substitution of derived flow parameters into the closed form boundary layer relations described above. At this stage then, the STC inviscid flow field has not been merged with the computed boundary layers.

The merging process is accomplished by restarting the program using the computed boundary layers from the first pass, and the flow near such boundaries is displaced accordingly. Several such restarts may be necessary before adequate convergence of the STC-SAB process is attained.

OUTLINE OF PROGRAM STEPS

The operations performed by the STC Program may be outlined as follows:

- (1) Define the flow regions and locate (approximately) the "primary" orthogonal and the streamlines which divide the internal and external flows.
- (2) Refine the grid as required by inserting additional streamlines and orthogonal lines between those already existing.
- (3) Compute the streamline angles and curvatures.
- (4) Compute the orthogonal line angles and move the grid points along the streamlines to obtain orthogonality.
- (5) Compute the velocities on the "far-field" boundary.
- (6) Adjust the flow rates in the exhaust streams, if any, to meet the calculated choking flow rate.
- (7) Integrate the momentum and continuity equations along each orthogonal [Eqs. (3.1) and (3.2)]. This step is also referred to as the "flow balance" calculation.
- (8) If the streamline positions are within a "rough tolerance", adjust the flow rate of variable flow channels to meet the "Kutta" condition at trailing edges. Step 7 is repeated with each iterative adjustment of the flow rates.
- (9) If the streamlines are within tolerance, return to step 2 for additional grid refinement (unless grid refinement limits have already

- been reached). Otherwise, continue to step 10.
- (10) Determine if the streamline positions are within final tolerance. If so, go to step 14. Otherwise continue to step 11.
 - (11) Set up the matrix equation for the streamline correction, δn .
 - (12) Solve the matrix equation.
 - (13) Modify the streamline position by δn , and return to step 3.
 - (14) Calculate and print the output quantities; calculate boundary layers and adjust wake table at trailing edges; then return to step 1 for the next case, or for SAB restart.

The first operation includes reading the input file for a description of the geometry and flow properties. The computer program has been written to have general capability for analyzing a great variety of configurations. The first step in the programmed logic is to develop a table of orthogonals or calculation stations for the several flow regions. The regions are determined as illustrated in Figure 3.2 so the calculation can proceed from upstream to downstream. The boundary of each region is defined as a primary orthogonal. As shown in Figure 3.2, the initial grid which is developed contains only the primary orthogonals and the double streamlines which separate the two illustrated flow channels.



Figure 3.2 Subdivision of Flow Field into Regions and Channels

For a full description of successive steps in the computational procedure refer to references 17 and 18.

4 THE DUCT ACOUSTICS FINITE ELEMENT PROGRAM

INTRODUCTION

The finite element method described here was first implemented by Abrahamson^{1,4,5}. It is based on the usual perturbation of the basic fluid mechanics equations for small motions with mean flow parameters derived in the absence of fluctuating quantities and then substituted into the equations for the acoustic quantities. These equations are linearized by neglecting higher order terms and the problem is reduced to two dimensions by assuming mean swirl to be zero and assuming a harmonic solution in the circumferential direction.

Originally, bilinear Serendipity isoparametric finite elements were used but the program has since been enhanced by the addition of subparametric Hermite elements. The original Serendipity elements are conforming and of type C^0 (that is preserving continuity of variables across element boundaries). The Hermite elements are nonconforming C^1 elements preserving continuity of variables and approximate continuity of their first derivatives across boundaries. (A discussion of the continuity characteristics of these elements is contained in the section on Element Derivation).

Element matrices are formulated using a Galerkin procedure and assembled in a rectangular mesh for which the matrix map is specifically coded. Nodal variables consist of the three complex components of acoustic velocity and (complex) acoustic pressure. In the case of Hermite elements, spatial derivatives of these physical parameters also become nodal variables. Nodal constants are the mean fluid parameters of density, velocity, and speed of sound.

The resulting assembled global matrix is a block tridiagonal system in which the blocks are themselves block tridiagonal. The system is non-Hermitian and non-positive definite and is solved by forward and backward substitution following an L-U decomposition with pivoting restricted internally to major blocks.

Since the solution of typical acoustic problems requires large solution grids and results in large demands on computer memory and central processor time, great attention has been paid to efficient memory management and efficient coding of computational operations. Use of the program has been simplified by the implementation of a fully automatic memory management scheme.

For completeness, the theory described in the references is summarized here with a detailed description of program operation in its current form.

DESCRIPTION OF THE MATHEMATICAL MODEL

Derivation of Equations

The nondimensional equations governing the motion of the fluid are:

Conservation of Momentum

$$\tilde{\rho} \left(\frac{\partial \tilde{V}}{\partial t} + (\tilde{V} \cdot \nabla) \tilde{V} \right) = -\nabla \tilde{p} + \frac{1}{Re} \nabla \cdot \underline{\underline{\tau}} \quad (4.1)$$

Conservation of Mass

$$\frac{\partial \tilde{\rho}}{\partial t} + \nabla \cdot (\tilde{\rho} \tilde{V}) = 0 \quad (4.2)$$

Conservation of Energy

$$\begin{aligned} \tilde{\rho} \left(\frac{\partial \tilde{T}}{\partial t} + \tilde{V} \cdot \nabla \tilde{T} \right) - (\gamma - 1) \left(\frac{\partial \tilde{p}}{\partial t} + \tilde{V} \cdot \nabla \tilde{p} \right) \\ = \frac{1}{Re} \left(\frac{1}{Pr} \nabla \cdot (\kappa \nabla \tilde{T}) + (\gamma - 1) \Phi \right) \end{aligned} \quad (4.3)$$

Equation of State

$$\gamma \tilde{p} = \delta \tilde{T} \quad (4.4)$$

Where ρ , \tilde{V} , \tilde{p} , \tilde{T} , Φ , $\underline{\underline{\tau}}$ are nondimensional density, velocity vector, pressure, temperature, dissipation function, and viscous stress tensor, respectively; γ and κ are gas specific heat ratio and thermal conductivity, and Re and Pr are Reynolds and Prandtl numbers.

Equations (4.1) through (4.4) were made nondimensional for simplicity by using an arbitrary characteristic length; the ambient values of temperature, density, and speed of sound; and arbitrary characteristic values of viscosity and thermal conductivity. These equations govern both the mean flow and imposed acoustic motion within the duct.

Although viscosity and dissipation were considered in deriving the mean flow, these influences were not considered in the acoustic equations. Thus, we write equations (4.1) and (4.2) in dimensional component form in cylindrical coordinates (ignoring viscosity) and assuming that all dependent variables are the sum of two motions, one the steady mean flow and the other a fluctuating acoustic motion, perturb these equations and subtract the unperturbed equations.

Neglecting second order terms in the fluctuating quantities, assuming mean swirl to be zero, we get a set of first order equations in the fluctuating, or acoustic, quantities.

The neglect of viscosity and heat conduction in the acoustic motion means that it is an adiabatic process. When such is true, the energy equation and

equation of state may be manipulated to give

$$p' = \rho' c^2 \quad (4.5)$$

Here c is the local speed of sound which is determined from the mean flow and p' and ρ' are acoustic pressure and density, respectively.

Using equation (4.5) to eliminate ρ' and taking a harmonic solution in time (t) and angle (θ) for the acoustic quantities,

$$(u', v', w', p') = (u, v, w, p) e^{\omega t + m\theta}$$

where ω and m are pure imaginary. The four equations governing the linearized acoustic motion in a nonuniform axisymmetric duct become

$$\omega u + \left(v + \frac{p\bar{V}}{\rho c^2} \right) \frac{\partial \bar{u}}{\partial r} + \bar{V} \frac{\partial u}{\partial r} + \left(u + \frac{p\bar{U}}{\rho c^2} \right) \frac{\partial \bar{u}}{\partial z} + \bar{U} \frac{\partial u}{\partial z} + \frac{1}{\rho} \frac{\partial p}{\partial z} = 0. \quad (4.6)$$

$$\omega v + \left(v + \frac{p\bar{V}}{\rho c^2} \right) \frac{\partial \bar{v}}{\partial r} + \bar{V} \frac{\partial v}{\partial r} + \left(u + \frac{p\bar{U}}{\rho c^2} \right) \frac{\partial \bar{v}}{\partial z} + \bar{U} \frac{\partial v}{\partial z} + \frac{1}{\rho} \frac{\partial p}{\partial r} = 0 \quad (4.7)$$

$$\omega w + \bar{V} \left(\frac{\partial w}{\partial r} + \frac{1}{r} w \right) + \bar{U} \frac{\partial w}{\partial z} + \frac{m}{\rho r} p = 0 \quad (4.8)$$

$$\begin{aligned} \frac{\omega p}{c^2} + \frac{\bar{U}}{c^2} \left(\frac{\partial p}{\partial z} - \frac{2p}{c} \frac{\partial c}{\partial z} \right) + \frac{\bar{V}}{c^2} \left(\frac{\partial p}{\partial r} - \frac{2p}{c} \frac{\partial c}{\partial r} \right) + u \frac{\partial \bar{p}}{\partial z} + v \frac{\partial \bar{p}}{\partial r} \\ + \bar{p} \left(\frac{\partial u}{\partial z} + \frac{\partial v}{\partial r} + \frac{m}{r} w + \frac{v}{r} \right) + \frac{p}{c^2} \left(\frac{\partial \bar{u}}{\partial z} + \frac{\partial \bar{v}}{\partial r} + \frac{\bar{v}}{r} \right) = 0 \end{aligned} \quad (4.9)$$

In these equations \bar{U} , \bar{V} , \bar{W} and u , v , w are the mean and acoustic velocity components in the z , r , θ directions, respectively. \bar{P} and $\bar{\rho}$ represent mean pressure and density and p is acoustic pressure.

Solution Strategy

Two principal decisions in the adoption of a solution strategy were the use of a finite element algorithm and the choice of a uniform rectangular discretization mesh.

A uniform rectangular discretization mesh does not imply that the grid points are to be equally spaced, or that the physical region should be rectangular. What it does imply is that there exists a simple mapping between nodes in a uniform rectangular mesh and nodes in an irregular nonuniformly discretized region.

The utility of this choice of a discretization mesh lies in the fact that it gives rise to an invariant global matrix map which may be explicitly embodied in a computer code for simplicity and efficiency.

A uniform discretization mesh for a duct of constant cross-sectional area is shown in Figure 4.1(a). The matrix map generated for this discretization by a nodal numbering system such as that shown in the figure is developed below. Within each of the linear elements, interactions among nodal variables will only occur between those variables at the corners of the rectangle. Thus in element (2, 4), four sets of linear equations will link the four sets of nodal variables located at nodes 14, 15, 24, and 25. Consider the equation set representing variables at node 25. On assembly of the global matrix, this set will contain contributions from four adjacent elements namely (2, 4), (2, 5), (3, 4), (3, 5). That is, in the global matrix, the variables at node 25 will be linked explicitly with variables at nodes 14, 15, 16, 24, 26, 34, 35, 36. All other coefficients in the submatrix, representing the equation set for variables at node 25, will be zero. For the case of "2" parameters per node, the matrix map generated by linear elements and the rectangular discretization numbered as shown in Figure 4.1(a), is given in Figure 4.2.

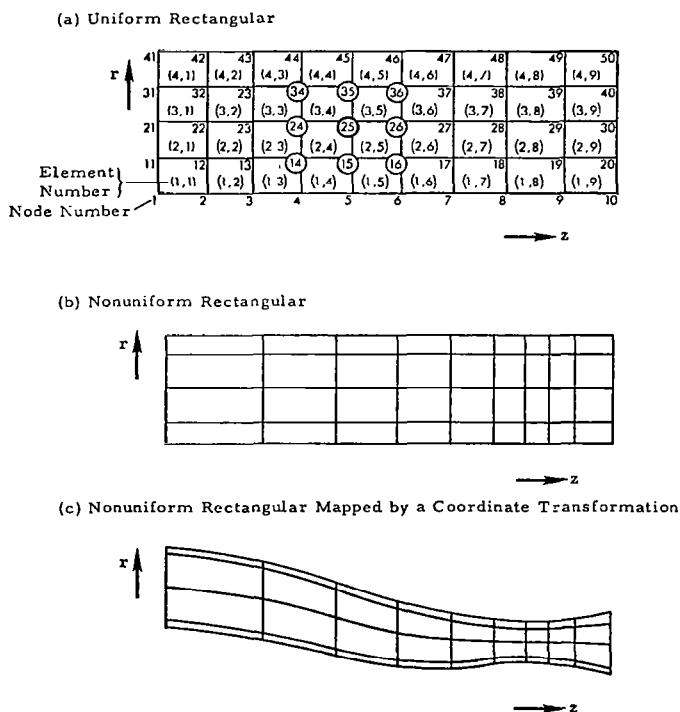


Figure 4.1 Rectangular Discretization in a Plane.

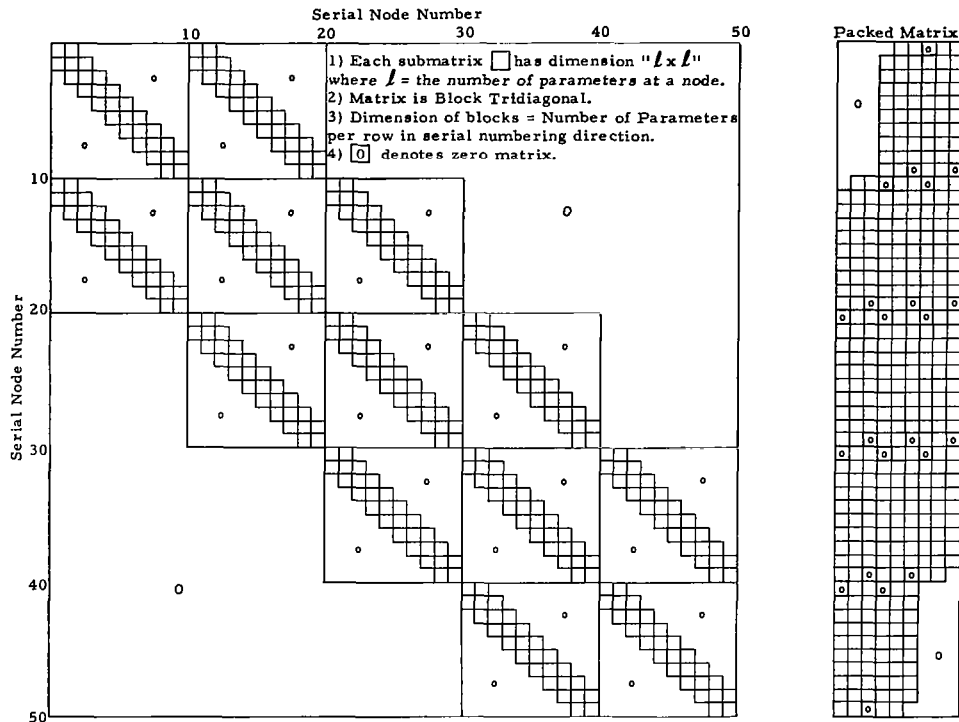


Figure 4.2 Matrix Map of the 2-D Rectangular Discretization of Figure 4.1

The principal generalized characteristics evident from the map shown in Figure 4.2 may be summarized as follows:

- Global matrix consists of three diagonal bands.
- Width of each band is " $3l$ ".
- Global matrix is block tridiagonal.
- Major blocks are themselves block tridiagonal.
- Order of major blocks is " nl ", where " n " is equal to the number of nodes per row in the serial numbering direction.
- Order of minor blocks is " l ".

Note that an identical matrix map will be generated by the nonuniform discretizations in Figures 4.1(b) and 4.1(c).

Element Derivation

The choice of a uniform rectangular discretization mesh imposes the requirement of a four-noded rectangular finite element as shown in Figure 4.3.

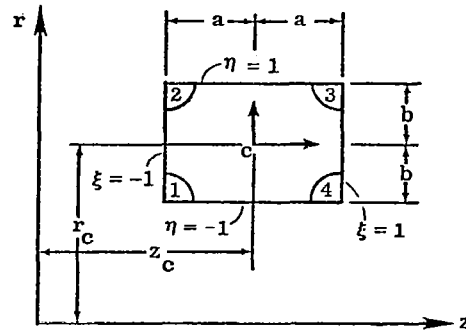


Figure 4.3 Rectangular Four-Noded Finite Element

To allow this simple shape to conform to complicated boundaries, a linear transformation of the global coordinates is applied:

$$\begin{aligned}
 r &= (N_1, N_2, N_3, N_4) \begin{Bmatrix} r_1 \\ r_2 \\ r_3 \\ r_4 \end{Bmatrix} = (N)\{r\} \\
 z &= (N_1, N_2, N_3, N_4) \begin{Bmatrix} z_1 \\ z_2 \\ z_3 \\ z_4 \end{Bmatrix} = (N)\{z\}
 \end{aligned}
 \tag{4.10}$$

where the (r_k, z_k) , $k = 1$ to 4 are the global coordinates of the four corners. The functions N_k are given by expressions of the form:

$$N_k = \frac{1}{4} (1 + \xi \xi_k) (1 + \eta \eta_k)
 \tag{4.11}$$

where values of (ξ_k, η_k) are fixed as $(-1, -1)$, $(1, -1)$, $(1, 1)$, $(-1, 1)$ 1 to 4, respectively.

Within the deformed region, the mean fluid parameters $\bar{\rho}$, \bar{U} , \bar{V} , \bar{c} of equations (4.6) through (4.9) are also defined by relations of the type in equation (4.10). For example,

$$\bar{U} = (N_1, N_2, N_3, N_4) \begin{Bmatrix} \bar{U}_1 \\ \bar{U}_2 \\ \bar{U}_3 \\ \bar{U}_4 \end{Bmatrix} = (N) \{\bar{U}\} \quad (4.12)$$

Thus the element geometry and mean flow parameters are expressed in terms of nodal values and element local coordinates η and ξ .

Derivatives of the mean flow parameters are obtained as follows:

$$\begin{Bmatrix} \frac{\partial N_i}{\partial \xi} \\ \frac{\partial N_i}{\partial \eta} \end{Bmatrix} = \begin{bmatrix} \frac{\partial z}{\partial \xi} & \frac{\partial r}{\partial \xi} \\ \frac{\partial z}{\partial \eta} & \frac{\partial r}{\partial \eta} \end{bmatrix} \begin{Bmatrix} \frac{\partial N_i}{\partial z} \\ \frac{\partial N_i}{\partial r} \end{Bmatrix} = [J] \begin{Bmatrix} \frac{\partial N_i}{\partial z} \\ \frac{\partial N_i}{\partial r} \end{Bmatrix}$$

where $[J] = \begin{bmatrix} J_1 & J_2 \\ J_3 & J_4 \end{bmatrix}$ = the Jacobian matrix.

$$\text{We may now define the matrix } \begin{Bmatrix} (\alpha_z) \\ (\alpha_r) \end{Bmatrix} = \begin{Bmatrix} \frac{\partial}{\partial z}(N) \\ \frac{\partial}{\partial r}(N) \end{Bmatrix} = [J]^{-1} \begin{Bmatrix} \frac{\partial}{\partial \xi}(N) \\ \frac{\partial}{\partial \eta}(N) \end{Bmatrix} \quad (4.13)$$

Thus for example,

$$\frac{\partial \bar{U}}{\partial z} = (\alpha_z) \{\bar{U}\} \quad (4.14)$$

The acoustic variables u, v, w, p within the finite element are given in terms of Hermitian functions of position and the values of the variables are as well as their derivatives at the nodes. For example, consider the variable u ,

$$u = \sum_{k=1}^4 \left\{ {}_1M_k u_k + {}_2M_k \left(\frac{\partial u}{\partial \xi} \right)_k + {}_3M_k \left(\frac{\partial u}{\partial \eta} \right)_k + {}_4M_k \left(\frac{\partial^2 u}{\partial \xi \partial \eta} \right)_k \right\} \quad (4.15)$$

where

$$\begin{aligned} {}_1M_k &= H_{0m}(\xi) H_{0n}(\eta) \\ {}_2M_k &= H_{1n}(\xi) H_{0n}(\eta) \\ {}_3M_k &= H_{0m}(\xi) H_{1n}(\eta) \\ {}_4M_k &= H_{1m}(\xi) H_{1n}(\eta) \end{aligned} \quad (4.16)$$

and where the indices m and n take on the following values depending on the node index "k":

k	m	n
1	0	0
2	0	0
3	1	1
4	1	0

and

$$\begin{aligned}
H_{00}(s) &= 1-3s^2+2s^3 \\
H_{01}(s) &= s^2(3-2s) \\
H_{10}(s) &= 2s(s-1)^2 \\
H_{11}(s) &= 2s^2(s-1)
\end{aligned} \tag{4.17}$$

$$\text{where } s = \frac{1}{2}(\xi+1) \text{ or } s = \frac{1}{2}(\eta+1) \tag{4.18}$$

Expressions of the type in equation (4.15) are inadequate for a finite element representation, however, since the nodal variables $(\frac{\partial u}{\partial \xi})_k$, $(\frac{\partial u}{\partial \eta})_k$, $(\frac{\partial^2 u}{\partial \xi \partial \eta})_k$ are referenced to local coordinates η and ξ . They may be expressed with respect to global coordinates as follows:

$$(\frac{\partial u}{\partial \xi})_k = J_{1k}(\frac{\partial u}{\partial z})_k + J_{2k}(\frac{\partial u}{\partial r})_k \tag{4.19}$$

$$(\frac{\partial u}{\partial \eta})_k = J_{3k}(\frac{\partial u}{\partial z})_k + J_{4k}(\frac{\partial u}{\partial r})_k \tag{4.20}$$

$$\begin{aligned}
(\frac{\partial^2 u}{\partial \xi \partial \eta})_k &= J_{2k}J_{4k}(\frac{\partial^2 u}{\partial r^2})_k + J_{1k}J_{3k}(\frac{\partial^2 u}{\partial z^2})_k \\
&+ (J_{2k}J_{3k}+J_{1k}J_{4k}) (\frac{\partial^2 u}{\partial z \partial r})_k
\end{aligned} \tag{4.21}$$

where the subscript "k" is used in every case to imply the value of the parameter at node k.

Substituting equations (4.19) through (4.21) into equation (4.15) gives the final expression for the variables within the finite element:

$$\begin{aligned}
u &= \sum_{k=1}^4 \left\{ M_k u_k + (J_{2k} M_k + J_{4k} M_k) (\frac{\partial u}{\partial r})_k + (J_{1k} M_k + J_{3k} M_k) (\frac{\partial u}{\partial z})_k \right. \\
&+ M_k \left. \left(J_{2k} J_{4k} (\frac{\partial^2 u}{\partial r^2})_k + J_{1k} J_{3k} (\frac{\partial^2 u}{\partial z^2})_k + (J_{2k} J_{3k} + J_{1k} J_{4k}) (\frac{\partial^2 u}{\partial z \partial r})_k \right) \right\} \tag{4.22}
\end{aligned}$$

(Note that in the above expressions, the M_k 's only are functions of ξ and η .)

Writing (4.22) as,

$$u = (M) \left\{ \begin{array}{l} \left\{ \begin{array}{l} u \\ u_{,r} \\ u_{,z} \\ u_{,r,z} \\ u_{,r} \\ u_{,z} \end{array} \right\}_{k=1} \\ \left\{ \begin{array}{l} u \\ u_{,r} \\ u_{,z} \\ u_{,r,z} \\ u_{,r} \\ u_{,z} \end{array} \right\}_{k=2} \\ \vdots \end{array} \right\} = (M) \{u_{,j}\} \quad (4.23)$$

where the notation $\{u_{,j}\}$ is used to represent u and its derivatives at all four element nodes. We may define a matrix similar to (4.13):

$$\left\{ \begin{array}{l} (\beta_z) \\ (\beta_r) \end{array} \right\} = \left\{ \begin{array}{l} \frac{\partial}{\partial z} (M) \\ \frac{\partial}{\partial r} (M) \end{array} \right\} = [J]^{-1} \left\{ \begin{array}{l} \frac{\partial}{\partial \xi} (M) \\ \frac{\partial}{\partial \eta} (M) \end{array} \right\} \quad (4.24)$$

So that for example,

$$\frac{\partial u}{\partial z} = (\beta_z) \{u_{,j}\} \quad (4.25)$$

Some discussion of the above expressions is helpful. In the rectangular element deformed with the η - ξ axis parallel to the r - z axis, $J_{2k} = J_{3k} = 0$ for all values of k , and the contributions of nodal parameters $(u_{,r})$ and $(u_{,z})$ are zero.

Also, in this special case, continuity of derivatives $u_{,r}$ and $u_{,z}$ across element boundaries is preserved. This is not the case with any other element deformation and in general continuity of derivatives normal to element boundaries is not preserved, although it always exists, of course, along element boundaries.

Since solution of equations (4.6) through (4.9) requires continuity only of the variables themselves, it is thus possible to vary the number of nodal derivatives in (4.23) from 1 to 6. This option has been implemented in the computer program with the most commonly used options being 1, 3, or 4, yielding, respectively, a pseudolinear element, a nonconforming Hermite element, and a conforming Hermite element for uniform area ducts.

Applying the Galerkin version of the method of weighted residuals, we may integrate equations (4.6) through (4.9) over an element. This is performed numerically using a Gaussian quadrature scheme in the simple undistorted local coordinate system. An element of area expressed in the local coordinate system is given by

$$dA = |J| \, d\eta \, d\xi \quad (4.26)$$

where $|J|$ is the determinant of the Jacobian matrix. Equations (4.6) through (4.9) thus become:

$$\begin{aligned}
& \int_0^{2\pi} \int_{-1}^{+1} \int_{-1}^{+1} (N)\{r\}\{M\} \left([\omega + (\alpha_z)\{\bar{U}\}](M) + (N)\{\bar{V}\}(\beta_r) \right. \\
& + (N)\{\bar{U}\}(\beta_z), (\alpha_r)\{\bar{U}\}(M), 0, \frac{1}{(N)\{\bar{\rho}\}} \left[\frac{(\alpha_r)\{\bar{U}\}(N)\{\bar{V}\}}{[(N)\{c\}]^2} \right. \\
& \left. \left. + (N)\{\bar{U}\}(\alpha_z)\{\bar{U}\} \right] (M) + (\beta_z) \right] \left. \right) \begin{pmatrix} \{u,\} \\ \{v,\} \\ \{w,\} \\ \{p,\} \end{pmatrix} |J| \, dnd\xi d\theta = 0 \quad (4.27)
\end{aligned}$$

$$\begin{aligned}
& \int_0^2 \int_{-1}^{+1} \int_{-1}^{+1} (N)\{r\}\{M\} \left((\alpha_z)\{\bar{V}\}(M), [\omega + (\alpha_r)\{\bar{V}\}](M) \right. \\
& + (N)\{\bar{V}\}(\beta_r) + (N)\{\bar{U}\}(\beta_z), 0, \frac{1}{(N)\{\bar{\rho}\}} \left[\frac{(N)\{\bar{V}\}(\alpha_r)\{\bar{V}\}}{[(N)\{c\}]^2} \right. \\
& \left. \left. + (N)\{\bar{U}\}(\alpha_z)\{\bar{V}\} \right] (M) + (\beta_r) \right] \left. \right) \begin{pmatrix} \{u,\} \\ \{v,\} \\ \{w,\} \\ \{p,\} \end{pmatrix} |J| \, dnd\xi d\theta = 0 \quad (4.28)
\end{aligned}$$

$$\begin{aligned}
& \int_0^{2\pi} \int_{-1}^{+1} \int_{-1}^{+1} (N)\{r\}\{M\} \left(0, 0, \left[\omega + \frac{(N)\{\bar{V}\}}{(N)\{r\}} \right] (M) + (N)\{\bar{V}\}(\beta_r) \right. \\
& + (N)\{\bar{U}\}(\beta_z), \frac{m_\theta}{(N)\{r\}(N)\{\bar{\rho}\}}(M) \left. \right) \begin{pmatrix} \{u,\} \\ \{v,\} \\ \{w,\} \\ \{p,\} \end{pmatrix} |J| \, dnd\xi d\theta = 0 \quad (4.29)
\end{aligned}$$

$$\begin{aligned}
& \int_0^2 \int_{-1}^{+1} \int_{-1}^{+1} (N)\{r\}\{M\} \left((\alpha_z)\{\bar{\rho}\}\{M\} + (N)\{\bar{\rho}\}\{\beta_z\}, \left[(\alpha_r)\{\bar{\rho}\}\right. \right. \\
& \left. \left. + \frac{(N)\{\bar{\rho}\}}{(N)\{r\}} \right] \{M\} + (N)\{\bar{\rho}\}\{\beta_r\}, \frac{m_\theta(N)\{\bar{\rho}\}\{M\}}{(N)\{r\}}, \frac{1}{(N)\{c\}^2} \left[\left[(\alpha_z)\{\bar{U}\} + (\alpha_r)\{\bar{V}\} \right. \right. \right. \\
& \left. \left. \left. + \frac{(N)\{\bar{V}\}}{(N)\{r\}} + \omega - \frac{2}{(N)\{c\}} \left[(N)\{\bar{U}\}(\alpha_z)\{c\} + (N)\{\bar{V}\}(\alpha_r)\{c\} \right] \right] \right] \{M\} + (N)\{\bar{U}\}\{\beta_z\} \\
& \left. \left. + (N)\{\bar{V}\}\{\beta_r\} \right] \right) \begin{pmatrix} \{u,\} \\ \{v,\} \\ \{w,\} \\ \{p,\} \end{pmatrix} |J| \, dnd\xi d\theta = 0 \quad (4.30)
\end{aligned}$$

Global Matrix Assembly and Boundary Conditions

Assembly of a global matrix equation, that is, a matrix equation representing the entire system, from a set of finite element matrix equations is a basic procedure in the finite element technique. Appropriate shifting of rows and columns are all that is required to add the local element matrix directly into the global matrix which is held in packed form (shown to the right in Figure 4.2) partially in direct access memory and partially on disk storage.

Along the outer boundaries of the discretized region, several different kinds of boundary conditions may exist. The current procedure for incorporation of boundary conditions is the direct insertion into the global matrix of an equation representing the condition imposed on the boundary nodal variables. This procedure is standard practice in finite element methodology, but has been shown²⁰⁻²² under some circumstances, to yield inferior results to the "natural" procedure for imposition of boundary conditions. The disadvantage with the natural procedure is that boundary conditions are satisfied only in an integral sense over the boundary. Alternate procedures to both methods have been suggested, for example see the "characteristic correction" of Gottlieb et al²³. These various techniques of imposing impedance boundary conditions are currently under review and alternate methods may be made available in the model.

Also, under review is the procedure of applying noise "source" conditions by setting nodal pressure or velocity variables to a specified value. Here the specified value includes reflected as well as incident energy and separation of these requires additional analysis. The modal source and radiation conditions also presented in references 20 through 22 appear to offer a viable alternative to the current procedure and should soon be implemented in the model.

PROGRAM STRUCTURE

Overview

It is becoming generally accepted within the discipline of computer science that the best manner of presenting detailed documentation of a computer code is within the code itself. Accordingly, the acoustic finite element code is heavily commented with definitions of variable names, delineation of functional blocks and explanations of procedures being implemented.

In contrast, the presentation given here describes the philosophy and overall structure of the program and is intended as an introduction for the general reader and programmer alike.

The program is divided into four phases, namely,

- Data input, determination of memory structure, and memory management.
- Recovery and interpolation of aerodynamic data generated by the GE-STC Program.
- Preparation of an output file for receipt of results from the acoustic finite element analysis.
- Execution of the acoustic finite element code. This involves two basic steps:
 1. Assembly and storage (on a disk file) of the global matrix equation.
 2. Reading global matrix (in portions from the disk file) followed by L-U decomposition and solution by forward and backward substitution.

Memory Management and Input Data Structure

Operation of the program is controlled by an executive which manages the subdivision of direct access memory into arrays for data storage. This procedure is very important in ensuring efficient use of memory and in permitting discretization grids of adequate size, since different phases of the program require different memory subdivisions.

The procedure which is used is based on a principle embodied in the FORTRAN language whereby arrays are passed from a calling segment to a subroutine by a starting address only.

Thus, using data input by the user, the executive calculates a memory subdivision for each phase of the program. A Control Data Utility - Common Memory Manager - is directed to provide the required additional space, and array starting addresses are passed to subroutines for execution of each phase of the program. (This procedure is facilitated but not dependent upon Common Memory Manager. If this utility is not available on a particular computer installation,

then the required additional space must be provided explicitly by the user in "Blank Common".)

Program input is described in detail in section 6, and consists of a data specification subroutine and six user-supplied FORTRAN functions. These functions describe spatial variations in the density of the discretization, as well as admittance, source and radiation boundary conditions.

Recovery and Interpolation of Aerodynamic Data

Phase 2 of the program (embodied in subroutine AEROPRE) reads duct geometry and aerodynamic data from the random access file prepared by the GE-STC program. The aerodynamic data are, of course, defined on the mesh generated by the STC mean flow solution algorithm. Since this mesh contains partial streamlines and partial orthogonal lines, the logic for interpolation to the acoustic mesh needs careful implementation. Because the acoustic mesh has parallel radial lines, the method used consists simply of specifying the axial coordinate of one of these lines and interpolating along all streamlines defined there. At each acoustic axial station this yields a set of values unequally spaced in radial coordinate (r). Interpolation at specified points along these radial lines yields the acoustic mesh.

Flow data output by the GE-STC program has not yet been merged with boundary layer flow profiles. This is performed subsequent to interpolation in AEROPRE by subroutine BNDLAYR and function BLPFILE using subroutine BLNORM, from boundary thickness (δ) data read from the GE-STC file. A one-seventh power boundary layer profile is applied to local Mach number so that the Mach number reaches .99 of its free stream value at a normal distance of δ from the wall.

Since mean flow temperature, pressure, density and the local speed of sound are all derivable from Mach number, ambient static pressure, and temperature, only Mach number and flow angle are interpolated and stored in array AERODAT. This array is retained in direct access memory throughout execution of the program. Subroutine AERO computes other mean flow parameters as required.

Coordinates of the acoustic mesh are not stored but are computed as required from boundary coordinate data arrays by subroutine COORDS.

Preparation of Output File

Due to severe restrictions on direct access memory during the solution phase of the AFE program, the task of preliminary preparation of the output file for interactive graphics is performed somewhat out of sequence. The interactive graphics program requires the coordinates of the acoustic mesh and also Jacobian matrices for each finite element in order to perform interpolations. These two sets of parameters are computed, blocked together, and written out to a mass storage file by subroutine OUTPRE.

Structure of the Finite Element Code

The first step in the AFE code involves numerical integration of the finite element equations (4.27) through (4.30) to produce local element matrices which are

$$x_k = a_k^{-1} \cdot (y_k - c_k x_{k+1}) \text{ for } k = n-1, 1$$

During assembly of the global matrix, the blocks are sparse and are packed in the manner described previously. During the solution phase "fill" is generated and an efficient minimum direct access memory configuration consists of three packed blocks, three block vectors and one expanded block. A description of the above operations using this memory configuration is given in Figure 4.5.

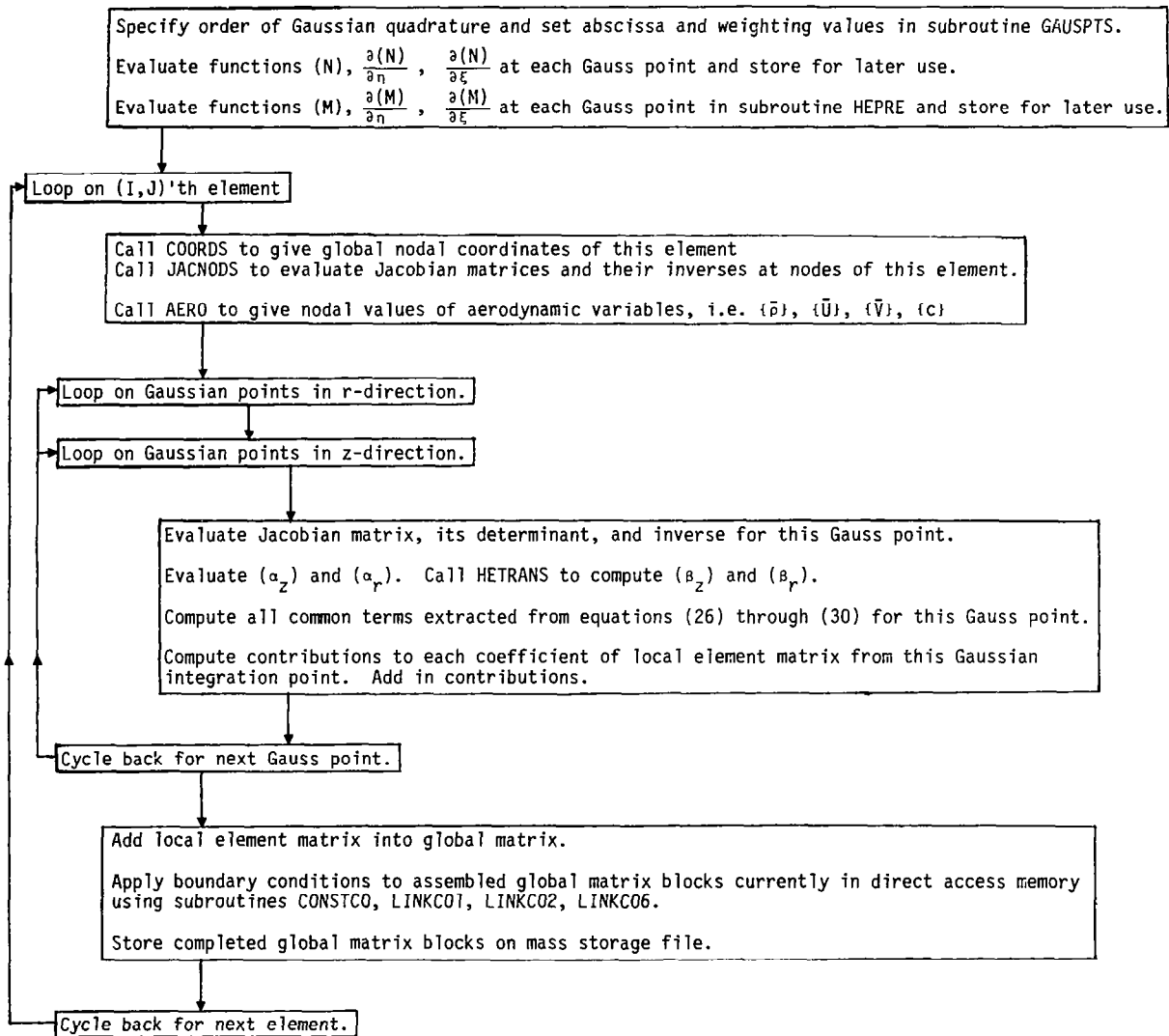


Figure 4.4 Functional Diagram for Numerical Integration of Finite Element Equations

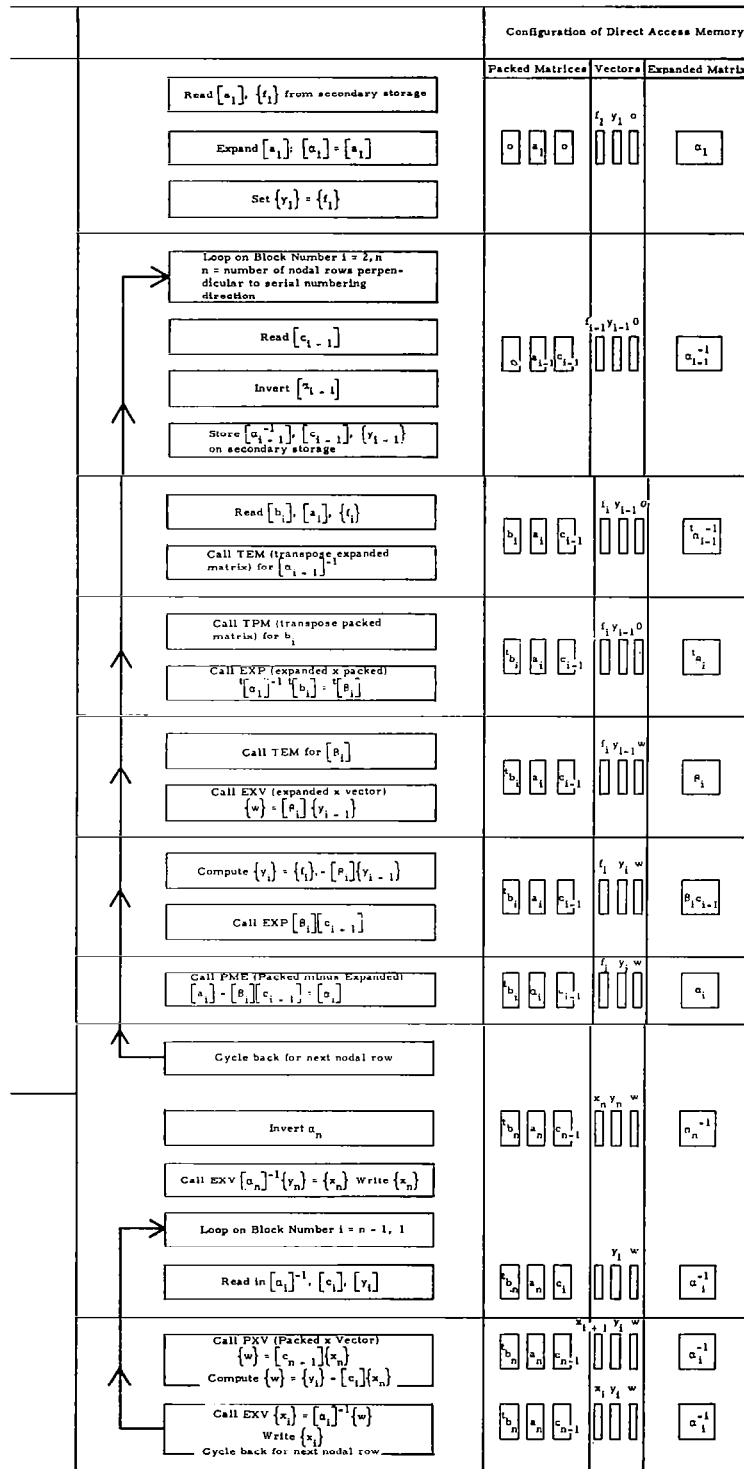


Figure 4.5 Description of Block Tridiagonal Matrix Solution with Memory Map

5 INTERACTIVE GRAPHICS PROGRAMS

INTRODUCTION

Both the GE-STC mean flow program and the acoustic finite element program produce large quantities of data, and in the case of both programs, it is necessary for the user to survey these data to satisfy himself as to the general "health" of the solutions over the entire domain.

For this reason alone, good graphics capability is essential. A predetermined off-line graphics process is cumbersome and does not give the necessary flexibility for close examination of interesting features or anomalies that might be noticed during a cursory review.

Interactive graphics, on the other hand, gives the user the capability to examine immediately an aspect of the solution behavior that might appear worthy of his attention. It is further possible to perform interactively, such functions as setting plot scales, adjusting the order of the interpolation between nodal values, or using the data to compute additional special parameters.

The facility also exists within the two graphics programs for interactively specifying off-line creation of permanent high quality plots for selected cases.

Flow Graphics Program

The principal utility of the flow graphics program is to enable an ADAM user to ascertain rapidly whether the mean flow data file created by the GE-STC program is satisfactory. The program is relatively simple in construct, calculates no additional functions from input aerodynamic data and produces only three basic plots. Contouring, which in itself is a sophisticated process, is performed by a standard library package.

The user may select contour intervals and plot scales and may examine selected areas of the flow field in detail.

Plot types produced by the program represent contour maps in the r - z plane of three selected variables:

- Those streamlines which are continuous over the required intervals.
- Mach number contours at user-specified intervals.
- Velocity contours at user-specified intervals.

Acoustic Graphics Program

The acoustic graphics program gives a user the capability to plot amplitude or phase of any acoustic variable (three components of acoustic velocity or pressure) along any nodal line in the finite element mesh. Nodal acoustic data generated by the AFE program are stored on a file whose format is described in

Appendix 2. This file also contains data titles, important input parameters from the GE-STC and AFE programs, AFE-mesh coordinates and finite element Jacobian matrices. Selected portions of this information may be displayed on the interactive terminal screen to avoid user errors in data file identification. Between nodes, interpolation is performed using the following relation:

$$u(\xi, \eta) = \sum_{k=1}^4 \{ {}_1M_k(\xi, \eta)u_k + (J_{2k} {}_2M_k(\xi, \eta) + J_{4k} {}_3M_k(\xi, \eta)) \left(\frac{\partial u}{\partial r}\right)_k + (J_{1k} {}_2M_k(\xi, \eta) + J_{3k} {}_3M_k(\xi, \eta)) \left(\frac{\partial u}{\partial z}\right)_k \}$$

taken from (4.22) with ${}_4M_k$ set to zero for element boundaries. Interpolations are performed in local (ξ, η) coordinates and transformed to global coordinates using the transformation,

$$r = (N) \{r_k\}$$

$$z = (N) \{z_k\}$$

where $(N) = \frac{1}{4} [(1-\xi)(1-\eta), (1-\xi)(1+\eta), (1+\xi)(1+\eta), (1+\xi)(1-\eta)]$

The sequence of operations carried out in the program are listed below with program segments performing these operations shown in parentheses:

1. Open random access file (MAIN) and read header records (RAHEADR)
2. Set up dynamic storage areas (MAIN)
3. Read nodal coordinates from random access file (RAINPT1)
4. (User) specify whether to switch to radial or axial plotting mode (MAIN)
5. For radial plots:
 - Read in function values at nodes for selected axial plane (RCIN)
 - Interpolate at user-specified radial locations for all available acoustic variables and compute admittance if this plane is a boundary (RINTERP).
 - Plot user-selected functions (RADPLOT) using NCAR graphics package (called from PLOTTR).
6. For axial plots:
 - Read in function values at nodes for selected radial nodal line (ACIN).

- Interpolate at user-specified axial locations for all available acoustic variables, acoustic flux, and complex admittance if this nodal line is a boundary (ZINTERP).
- Plot user-selected functions (AXPLOT) using NCAR graphics package (called from PLOTTR).

The National Center for Atmospheric Research (NCAR) graphics package referred to above creates a "metacode file" which contains all completed plots. Special routines in the NCAR package combined with a NASA-Langley utility TRN and Tektronix graphics routines translate this metacode file to a display on the Tektronix terminal screen.

Upon completion of an interactive plotting session, the user may direct TRN to access the NCAR "metacode file" and produce a "graphics command file" which is then accessed by an off-line batch stream job to produce permanent (CalComp) plots.

Note: To ensure that direct access memory requirements are held below the limits allowable for interactive processing at NASA-Langley, this program performs dynamic memory management using the CDC utility "Common Memory Manager". Dependence on this utility may affect its portability.

6 USERS' GUIDE

COMMENTS ON ADAM/NOS INTERFACE

A more detailed version of the simplified block diagram of the ADAM system contained in Figure 2.1 is given in Figure 6.1. This figure shows in addition to the principal functional steps and data files, the CDC-NOS (Network Operating System) interface. This interface consists of a set of procedures which greatly simplify the users task. Instructions on the use of these procedures are contained in this section for individual processes under the heading "Operation Under CDC-NOS".

Use of the system is strongly oriented towards interactive processes and in this context user ability to create, edit, and maintain NOS files is central to most operations. The principal tool for performance of these functions is the editor XEDIT. Manuals on NOS and XEDIT are available for users, from the NASA-Langley Analysis and Computation Division.

Although functions, such as the creation of input data files, and the examination of program output data are truly interactive, other processes are too consuming of computer resources and/or take too long to be performed interactively. These include executing the GE-STC program, executing the AFE program, and the creation of high quality (CalComp) hardcopy plots. These processes are executed as "batch" jobs after being created by a user at an interactive terminal and are sent by him to the computer of his choice for off-line processing.

Before executing ADAM NOS Procedures for the first time, a new user must get copies of these procedures (STCDECK, PROCPLT, AFEDECK, AFETDEK) saved under his user number and modified to include his own user and delivery information.

RUNNING THE GE-STC PROGRAM

Operation Under CDC-NOS

Prior to execution of the GE-STC program, a "namelist" input data file should be prepared as described in the following sections using data sheets contained in Appendix I.

To execute the program the user then issues the following commands at an interactive terminal

```
GET, STCRUN
```

```
STCRUN, DATIN = F1, DATOUT = F2, COMP = M.
```

where F1 = Name of user input data file

F2 = Name which the user wishes to give to the output data file which will be created by the program.

M = the letter name of the machine on which the user wishes the program to be executed.

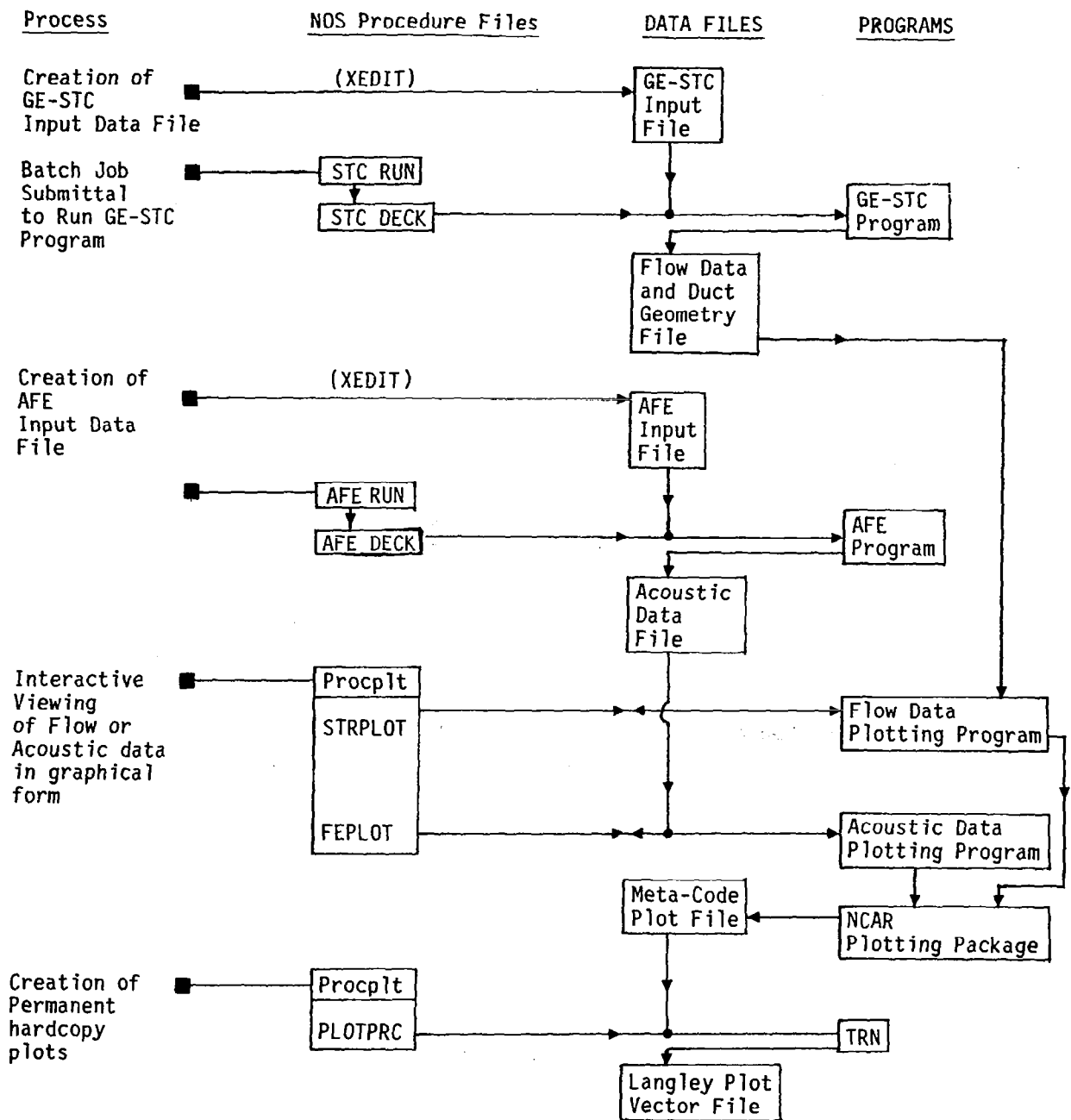


Figure 6.1 ADAM System Functional Diagram

Preliminary Comments on Input Data

Primary items of importance in trouble-free use of the GE-STC program are:

- Specification of Smooth Input Geometry - Since the STC method uses boundary surface curvature to compute velocity and pressure gradients, it is imperative that surface curvatures are piecewise continuous. Smooth boundaries are most easily accomplished by using analytic functions with continuous second derivatives.
- Grid Refinement Criteria - The purpose of grid refinement criteria is to maximize refinement in areas of large flow gradients while minimizing additional refinement in areas of smooth flow. Experience in program use will best assist the user in making optimum choices of refinement parameters when combined with the general guidelines in the following sections.
- Iteration Tolerances - These control the logic for grid refinement and "flow balance" in the inner loop solution. Satisfactory operation usually occurs using the preset values. Instability in streamline adjustment may occur when small tolerances are combined with high grid refinement resolution in a region of large streamline curvature. The remedy is to change tolerances, grid refinement or both. A good procedure is to keep iteration tolerances relatively large during grid development and then restart the last grid refinement with smaller tolerances.

The STC analysis has been set up as a user-oriented program and most control variables have been preset to generally useful values. If numerical difficulties do occur, they will invariably be related to geometry errors or bad judgement in selecting grid refinement or iteration tolerances.

INPUT DATA FOR THE GE-STC PROGRAM

The following explanatory notes are intended to assist the user in completing input data sheets for the GE-STC program which are contained in Appendix I. Although this program will cope with any consistent set of units, the Acoustic Finite Element Program expects values in the MKS system. Therefore, all input data should be specified in this system. (Note that values in parenthesis on the data sheets are default values to be used if no input is specified for particular parameters.)

Input Sheet 0

This consists of three lines of identification information in columns 2 through 61 listing user name, user location, and problem identification, respectively.

Input Sheet 1

STC: Restart Control Parameter - Partially refined grids may be read from or saved on files by specifying a "T" in either column 14 or 24. In

the former case, it is necessary only to specify those input quantities which differ from those originally input. Note that the final run of a problem with boundary layers introduced into a fully converged STC solution is always a restart case.

MACHO: Free stream Mach number

TSO, PSO: Ambient temperature (K), pressure (N/M^2)

RG, GAM: Gas constant J/(Kg.K), ratio of specific heats

RHL: Highlight radius (M) - A reference (or highlight) area ($= \pi(RHL)^2$, axisymmetric or $= RHL$, planar) to be used for defining the mass flow for each channel (see A0 sheet 3).

RM: Maximum body radius (M) - Computed pressure drag forces are normalized by max. body area ($= \pi(RM)^2$, axisymmetric, or $= RM$, planar).

TTE: Body closure tolerance (M) - Maximum trailing edge thickness.

AXI: Axisymmetric or planar (T or F).

Grid Refinement Criteria

The grid will be refined locally as required until the spacing of orthogonals and streamlines is less than the values given in the SGR and SGZ tables and the Mach number difference between any two points on a streamline or on orthogonal line is less than VMG1 and VMG2, respectively. As a guide, it is suggested that SGR be set to about twice the expected grid spacing.

GR: Radial values where SGR is to be specified (M).

SGR: Spacing of grid lines in radial direction (M).

NGR: Number of values of GR and SGR.

GZ: Axial values where SGZ is to be specified (M).

SGZ: Spacing of grid lines in axial direction (M).

NGZ: Number of values of GZ and SGZ.

VMG1,

VMG2: Maximum Mach number increment between grid points in streamline or orthogonal directions, respectively.

Iteration Tolerances

The solution method consists of constructing a grid of streamlines and orthogonal lines. Starting with two streamlines per channel (one for each boundary) and an orthogonal passing through the first and last point of each boundary, the grid is automatically refined by successively dividing grid intervals in half. The solution accuracy and computational cost are directly related to the extent of grid refinement. Provided MAXIT, the maximum number of refinements, is not exceeded the grid will be refined locally as previously specified by the grid refinement criteria.

- MAXIT: Maximum number of grid refinements.
- RHOC: Curvature damping - In some instances, it may be necessary to increase this parameter from its preset value of unity to a value of two or greater if an oscillation of MAXES2 is observed in the iteration history printout.
- NODENS: Number of streamline position refinements at constant density - At the default value of zero, the incompressible equations are used for the zeroth refinement only. At greater values (e.g. NODENS = 2) the inadvertant possibility of supersonic velocities occurring is prevented and is recommended for reliable starting. Where adjacent streams have large differences in total pressure (as in jet plume analysis), a value of -1 is recommended.

Boundary Layer Parameter

The following parameters define reference values for boundary layer computation.

- TREF: Reference temperature for viscosity solution (K)
- MUREF: Reference viscosity at TREF (J/Kg. K)
- SCON: Sutherland constant (K)

Optional Input

A large number of input quantities, in addition to those described above, may be specified. These items are not normally required for execution of the STC program and consist in general of controls for special program options and input data to modify preset or initialized constants or parameters.

A selected few of these optional input parameters are described in the addendum to Appendix 1. For a full list, the user is directed to Reference 17.

Input Sheet 2

Each input sheet 2 specifies data along one particular boundary. When preparing an aerodynamic data file for use by the AFE program, only two geometric boundaries are permitted, namely inner and outer duct walls. To get accurate estimates of flow for real engine nacelles, however, it is often necessary to perform preliminary STC program runs with several flow channels and multiple boundaries. For example, Figure 6.2 shows a case with three flow channels. Upon completion of the preliminary analysis, the positions of stagnation streamlines will be available. These may then be used as artificial boundaries for a single channel analysis for use by the AFE program.

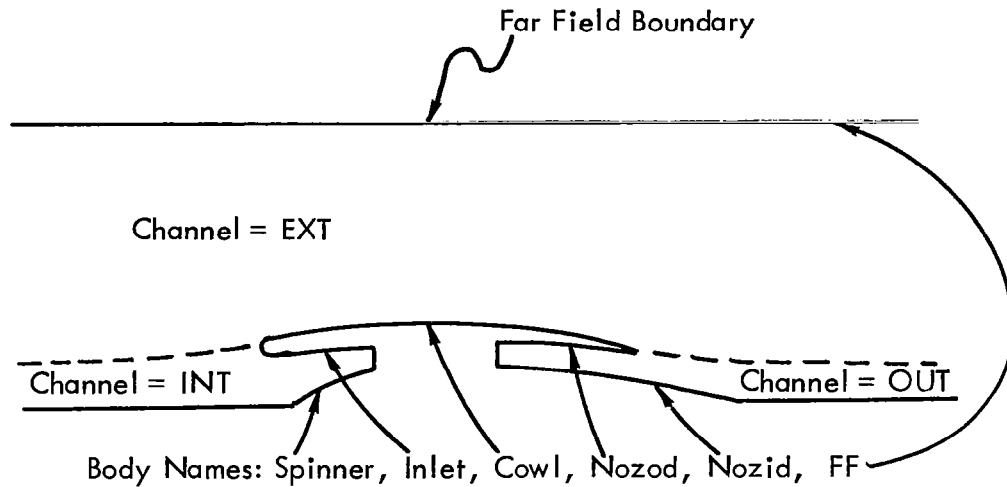


Figure 6.2: Illustration of a Multiple Channel Configuration

Each channel must be bounded, at least in part, by an upper boundary and a lower boundary. It is also possible for a channel geometric boundary contour to be composed of several physical boundaries. In this case, an input sheet must be completed for each physical boundary and end point coordinates must be identical. The AFE program will also recognize this situation and will perform correctly, linking physical boundaries to form a single geometric contour. Certain channel and boundary names are reserved by the program for particular uses as listed below.

Reserved Channel Names:

- EXT - External flow channel
- INT - Inlet flow capture channel

Reserved Boundary Names:

- FF Far field boundary. This name causes the numerical flow solution to be matched to a small perturbation analytical solution in the region from the far field boundary to infinity.
- PRES 1 } Up to two pressure boundaries are allowed permitting static pressure along a boundary to be specified by the user.
- PRES 2 }
- FREE1 } A free boundary is a constant pressure boundary which is downstream of a fixed boundary and has the same pressure as the last point on the fixed boundary.
- FREE2 }

Items listed on input sheet 2 are generally self explanatory. Boundary coordinates at sharp corners must be listed twice, one time for each angle which

exists at that point. In each interval, a locally rotated cubic polynomial is fitted by the program. Generally, it is extremely important that contours are smooth and points consistent with specified angles.

All points must be listed in the streamwise direction. For an inlet lip starting at the highlight, internal and external surfaces are listed separately with ANGD at the highlight equal to $+90^{\circ}$ for the external surface and -90° for the internal surface.

The format for specifying pressure boundaries or free boundaries is contained in input sheet 2a.

Boundary layer calculations on a particular surface, are normally specified using the input given on sheet 2. In some cases, it is desirable to introduce boundary layers into a fully converged STC inviscid solution. This may be conveniently done on restart using the procedure described in input sheet 3a.

Input Sheet 3

Data on input sheet 3 supplies entrance flow properties for each channel.

Total pressure and total temperature may be specified using one of the following procedures:

- Specify TTO and PTO if the stagnation properties are known.
- Specify MACHO, TSO and PSO if static properties and Mach number are known. If only MACHO is supplied, values from sheet 1 will be used for TSO and PSO.
- If no values are input, then free stream values from sheet 1 are used.

A0 is the channel area used for determining channel flow rate. It should be input as a fraction normalized by the highlight area calculated from RHL on sheet 1.

If for any channel input data are not supplied, the reference properties on sheet 1 will be used with frontal area computed at the entrance station. This option is suggested for an external stream.

Channel flow rates will normally be adjusted to meet trailing edge or choked flow conditions. If flow rate is not to be varied for this channel, set VARY = F.

An example of a typical input data file for the GE-STC program is contained in Appendix 1 following input data sheet blanks.

Interpretation of Program Output

Output from the STC program may be divided logically into the following eight

sections:

1. Input data file.
2. Input and calculated boundary coordinates and angles.
3. Printer plot of initial XI1, XI2 grid map.
4. Solution history.
5. General input and output data.
6. Flow field data along orthogonal lines.
7. Calculated flow data along field boundaries and final channel momentum balances.
8. Boundary layer data.

Only items 6, 7, and 8 will be described in detail, as the other items are best left to the reference. However, a few notes are in order. Problems arising in the use of this program can usually be attributed to incorrect specification of the initial or boundary conditions. A careful inspection of the calculated boundary quantities of section 2 will usually show a point or region of high curvature, which should be examined for correctness. Also, in the solution history, the behavior of MAXES2 relative to LIMES2 indicates convergence by a decreasing absolute value. Any erratic behavior in MAXES2 indicates convergence problems and the user is referred to notes in the addendum to Appendix 1 and to reference 17.

6 Flow Field Data Along Orthogonal Lines

A tabulation of column headings in the section of data output follows:

- XI1 - Orthogonal(station) numbering coordinate
- XI2 - Streamline numbering coordinate
- STRM FNCT - Dimensionless stream function (fraction of flow in channel).
- X,Z - Streamwise coordinate
- Y,R - Transverse or cross-stream coordinate
- PHI - Flow angle (degrees)
- CURV - Streamline curvature
- PS/P0 - Ratio of local static pressure to reference static pressure
- PS/PT - Ratio of local static pressure to total pressure
- TS/TT - Ratio of local static temperature to total temperature
- CP - Pressure coefficient
- MACH - Mach number
- Area - Flow area

PT/PT0 - Channel total pressure ratio

7 Calculated Flow Data along Field Boundaries and Final Channel Momentum Balances

SLW - Distance along boundary

XW,ZW - Axial coordinate

YW,ZW - Vertical or radial coordinate

ANGW - Flow angle or surface angle

CURVW - Streamline or surface curvature

Momentum Balance - The difference between the entering and leaving momentum may be interpreted as an indication of the accuracy of the analysis.

8 Boundary Layer Data

XW - Axial coordinate

THETA - Momentum thickness (θ)

DSTAR - Displacement thickness (δ^*)

DELTA - Boundary layer thickness (δ)

REX - Local Reynolds number

CAPX - Equivalent flat plate distance along surface

CF - Skin friction coefficient (C_f)

SW - Distance along surface (s)

DSTR - Smoothed displacement thickness (δ^*)

DDSTR - $d\delta^*/ds$

SEP - Separation flag, = SEP if separation occurs

F - Stratford separation parameter

USING THE FLOW GRAPHICS PROGRAM

Operation under NOS

After a random access mass storage file containing aerodynamic data from the

GE-STC program has been generated, it may be examined interactively by issuing the following commands from a Tektronix terminal:

```
GET, TAPE 11 = (filename of GE-STC output file)
GET, PROCPLT.
BEGIN, STRPLOT, PROCPLT.
```

The procedure FEPLLOT executes the GE-STC data graphics program and subsequently under user direction, may proceed to execute a post processor program to allow the user to obtain CalComp permanent plots via a batch job submittal.

The postprocessor program which creates the "Plot Vector File" at NASA-Langley is called TRN. The use of TRN for permanent plots from the flow graphics procedure is identical to its use by the acoustic graphics procedure and is described under that heading.

Notes for an Interactive Session

Throughout the interactive session, all user input is prompted by directions appearing on the screen.

For all user input, a "Y" indicates "yes" and "N" indicates "no". A blank or any other character is assumed to be "no".

Queries are self explanatory and when user input data are required they are checked to ensure that they fall within the valid range before proceeding.

The three plots are produced in sequence so that in order to repeat a particular plot, it is necessary to repeat the entire sequence.

When completing an interactive session, the user may enter the postprocessor program TRN. No prompting instructions are issued by TRN and the user is obliged to know the required command format.

RUNNING THE ACOUSTIC FINITE ELEMENT PROGRAM

Operation Under CDC-NOS

A convenient procedure has been devised for running the AFE program under the CDC-NOS operating system:

- Step 1 - Creation of a user-functions input file as described in the following section.
- Step 2 - Creation of a geometry and aerodynamic data file using the GE-STC program.
- Step 3 - At an interactive terminal, the user issues the following instructions:

GET,AFERUN.

AFERUN, FUNC = F1, AERO = F2, OUT = F3, COMP = M.

where F1 = User-functions file name.

F2 = The name of the output file which was created by the GE-STC Program.

F3 = The name which the user wishes to give to the output file which will be created by this run of the acoustic finite element program.

M = The letter name of the machine where the user wishes the program to be executed.

If the user desires a listing of the program or has made changes to the code, then the following instructions should be issued:

GET,AFETRUN.

AFETRUN,PROG = NAME, FUNC = F2, OUT = F3, COMP = M.

where "NAME" is the name of the new program source file.

The ADAM NOS procedures described above use the following files:

AFEDECK - The job deck which will be sent to the computer of the users' choice to run his job.

AFERUN - The interactive procedure to send the job to a batch processing stream. This procedure also performs a syntactic check on the user functions file, and checks to see whether the GE-STC file exists.

AFETDEK - The job deck to test run a new version of the AFE Program.

AFETRUN - The interactive procedure to send a test run to a batch processing stream. In addition to the actions performed by AFERUN, a syntactic check on the new version of the AFE program is also performed.

AFE12 - The program source file.

PBIN - The compiles relocatable binary file from the source file, AFE12.

Preparation of the User-Function File

User input to the AFE program consists of a FORTRAN subroutine and five FORTRAN functions.

Subroutine DATASUB - Specification of input variables.

Function ZPDFN - Axial points distribution

RPFN - Radial points distribution

ADMITO - Outer wall acoustic admittance

ADMITI - Inner wall acoustic admittance
 ADMITT - Admittance of duct termination
 PSOURCE - Pressure distribution over source plane

The FORTRAN subroutine DATASUB is simply a vehicle for transferring data into the program. This could have been equally specified as a data file but has been cast as a subroutine for consistency in format with other program input. In this way, a single file may be readily used for all input data.

The format of the data subroutine is shown in the following example:

```

SUBROUTINE DATASUB(M,NDUCT,ZLOCS,ZLOCR,FREQ,MSPIN,FLOW
1,AMPHAS, OUTFILE,BCWEAK,NNDERIV,IWRITE)
C
C   This subroutine contains input variables for program AFE12.
C
C   LOGICAL FLOW,AMPHAS,OUTFILE,BCWEAK
C
C   Set Program Input Variables:
C
C   M = No. of elements in radial direction
C
C   NDUCT = No. of axial elements in duct.
C   ZLOCS = Z-coordinate of source in GE-STC reference frame
C
C   ZLOCR = Z-coordinate of radiation boundary in GE-STC reference frame
C   FREQ = Source frequency in hertz
C
C   MSPIN = Circumferential (spinning) mode number
C           = 0 for axisymmetric case.
C
C   FLOW = .FALSE. for zero mean flow
C
C   AMPHAS = Output format indicator
C           = .TRUE. for output of nodal variables in amplitude and phase
C           = .FALSE. for output of nodal variables in real and imaginary
C
C   Outfile = .TRUE. for creation of output file containing analysis
C             results for use by interactive graphics program.
C
C   BCWEAK = .TRUE. for application of derivative wall boundary conditions
C            by subroutine LINK06.
C           = .FALSE. for successive applications of derivative wall boundary
C            conditions by subroutine LINK02.
C
C   NNDERIV = Number of nodal derivatives of each physical parameter
C            = 1 for linear elements
C            = 3 or 4 for Hermite elements
C

```

```

C      IWRITE = 0 for no printed output
C          1 for nodal variables only
C          2 for nodal variables + interpolated values in radial dirn.
C      DATA TITLE : PROGRAM TEST FOR GEDATA2
C          M = 11
C          NDUCT = 50
C          ZLOCS = 3.0
C          ZLOCR = 0.01
C          FREQ = 512.0
C          MSPIN = 0
C          FLOW = .TRUE.
C          AMPHAS = .TRUE.
C          OUTFILE = .TRUE.
C          BCWEAK = .FALSE.
C          NNDERIV = 3
C          IWRITE = 2
C          RETURN
C          END

```

Where lines beginning with a "C" are nonexecutable comments, explaining the function of input variables.

Variables "M" and "NDUCT" define the overall size of the mesh. The magnitude of M is limited by the size of direct access memory, whereas NDUCT is unlimited. Current limits to M on a Cyber 175 computer with just over 100k words of direct access memory is 46 linear elements or 12 Hermite elements.

Spacing of grid points in the axial and radial directions is controlled by points distribution functions ZPDFN and RPFN, respectively. These functions define curves of normalized coordinate distance versus point number.

For example, the following function specifies a uniformly spaced axial mesh by giving a linear relationship between ZPDFN (=Normalized axial coordinate) and axial point number J, where J varies from 1 to N+1. (Note that for N finite elements there exist N + 1 points).

```

      Function ZPDFN (J,N)
C
C      ZPDFN: Normalized axial (Z) points distribution function
C      J = Axial point number
C      N = Number of axial elements (= No. of points - 1)
C      ZPDFN = Normalized axial coordinate corresponding to point J
C
C      This is a linear points profile
C
C      ZPDFN = (J-1.0)/N
C      RETURN
C      END

```

More complicated distributions are frequently necessary. For example, analysis of a duct with flow containing a constriction in the central area of the analy-

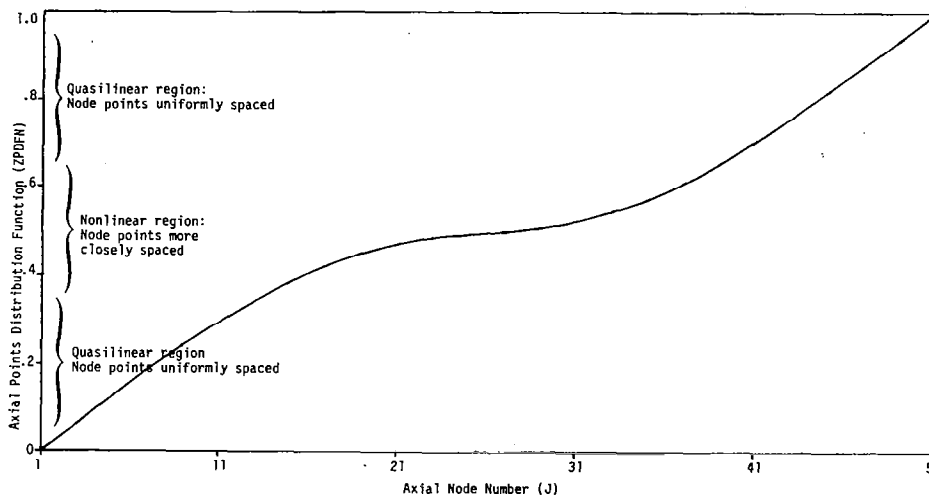
sis region requires a finer mesh spacing in the constriction region since acoustic wavelength decrease here for sound propagation against the mean flow.

The following function (illustrated in Figure 6.3 for $N = 50$) was used for this problem.

```

Function ZPDFN(J,N)
C
C ZPDFN: Normalized axial (Z) points distribution function
C J = Axial point number
C N = Number of axial elements (= No. of points - 1)
C ZPDFN = Normalized axial coordinate corresponding to Point J
C This is a non-uniform profile with points clustered about the center
C of the Z-coordinate range.
DATA PI/3.14159265/
JM1 = J-1
IF (JM1.GT.N/2.) GO TO 10
ZPDFN = 0.5*SIN (JM1*PI/N)
RETURN
ZPDFN = 0.5*(2.+SIN(-(N-JM1)*PI/N))
RETURN
END

```



6.3 Nonuniform Axial Points Distribution Function for Duct with Central Constriction

In the radial direction the presence of a boundary layer on the outer wall with large flow gradients requires a closer spacing of mesh points. A points distribution function specified explicitly for such a case with $M=11$ follows:

Function RPFN(I,M)

```
C
C RPFN - Normalized radial points distribution function
C I = Radial point number (input)
C M = Number of radial elements (input) (= No. Points - 1)
C RPFN = Normalized radial coordinate corresponding to Point I
C
C This is an example of a radial points profile with data specifically
C set for 11 radial elements.
C
DIMENSION DAT(12)
DATA DAT/0.0,.01,.1,.3,.5,.7,.9,.99,.999,.9999,.99999,1./
IF (M.NE.11) STOP 22
RPFN = DAT (I)
RETURN
END
```

In this profile, a single point is also placed close to the axis, although no boundary layer exists here, since this is often a region of large acoustic gradients.

A more general profile accomplishing a similar end to the previous case follows:

Function RPFN(I,M)

```
C
C RPFN = Normalized radial points distribution function
C I = Radial point number (input)
C M = Number of radial elements (input) (=No. Points - 1)
C RPFN = Normalized radial coordinate corresponding to Point I
C DIMENSION DI(3),DO(8)
C DATA DI/0.0,.005,.015/
C 1, DO/.96,.98,.993,.998,.9995,.99995,.999995,1.0/
C
C This DISTRIB FN. is composed of three segments with inner and outer
C segments specified explicitly and the middle segment being a linear
C division among remaining elements.
C
5 NI = 3
NO = 8
C NI, NO = Number of nodes in inner and outer distributions, respectively.
IF (I.GT.NI) GO TO 10
RPFN = DI(I)
RETURN
10 IF (I.LT.M-NO+2) GO TO 20
RPFN = DO(I-M+NO-1)
RETURN
C NC = Number of elements in central distribution
20 NC = M-NI-NO+2
RPFN = DI(NI) + (DO(1)-DI(NI))*(I-NI)/NC
RETURN
END
```


Complex nondimensional specific acoustic admittances on boundaries of the analysis region are specified by the three functions ADMITO, ADMITI, AND ADMITT. Here ADMITO refers to the outer wall boundary, ADMITI to the inner wall boundary for a coaxial duct, and ADMITT to the termination boundary. The format of these three functions is identical; all being dependent on a single nondimensional spatial variable. Note that the analysis employs the $e^{+j\omega t}$ convention so that when comparing admittances with analyses using the $e^{-j\omega t}$ convention, the sign of the imaginary part should be reversed. Note also that standard values of $\bar{\rho}$ and c are used in converting to dimensional admittances. These values are specified at the beginning of the program in MKS units.

A "hard wall" example of an admittance function follows:

```

      COMPLEX FUNCTION ADMITI(Z)
C
C   ADMITI = Specific acoustic admittance of inner walls
C   Z = Nondimensional axial distance (Range is from zero to one).
      ADMITI = CMPLX(0.0,0.0)
      RETURN
      END

```

An example of a "plane wave" radiation admittance ($= \frac{1}{\rho c}$) follows:

```

      COMPLEX FUNCTION ADMITT(R)
C
C   ADMITT = Specific acoustic admittance of duct termination
C   R = Nondimensional annular radial coordinate (= 0 at inner wall)
C
      ADMITT = COMPLX(1.0,0.0)
      RETURN
      END

```

The function PSOURCE allows the user to specify a complex pressure distribution over a radial plane at one end of the analysis region.

e.g.

```

      COMPLEX FUNCTION PSOURCE(R,MSPIN)
C
C   Function calculates pressure distribution at duct source
C   R = Nondimensional annular radial coordinate (= 0 at inner wall)
C                                           (= 1 at outer wall)
C
      PSOURCE = CMPLX(1.0,0.0)
      RETURN
      END

```

Note that this pressure distribution includes incident acoustic energy, as well as acoustic energy reflected back from the duct itself.

USING THE ACOUSTIC GRAPHICS PROGRAM

Operation Under NOS

After a random access mass storage file containing acoustic data from the AFE program has been generated, it may be examined interactively by issuing the following commands from a Tektronix terminal:

```
GET,TAPE11 = (filename of AFE output file)
GET, PROCPLT.
BEGIN, FEPLLOT, PROCPLT.
```

The procedure FEPLLOT executes the AFE data graphics program and subsequently under user direction, may proceed to execute a postprocessor program to allow the user to obtain CalComp permanent plots via a batch job submittal.

The postprocessor program which creates the "Plot Vector File" at NASA Langley is called TRN. Its input is prompted by "TRN>" on the screen. A document "Introduction to TRN" may be obtained interactively as follows:

```
GET, TRNDOC/UN = 973650N.
```

Related files in this section of the ADAM system are:

```
FEPLFOR - Interactive graphics program source file.
FEPLTAB - Compiled binary executable file of FEPLFOR.
```

Guide to a Typical Interactive Session

Throughout the interactive session, all user input is prompted by directions appearing on the screen. Since these directions are self-explanatory, these notes are brief.

The first action of the program is to write titles and a list of data-identifying parameters on the screen. These are obtained from the AFE data file and relate to both GE-STC program input parameters and AFE program input parameters.

The user is then given the option of verifying AFE-mesh nodal coordinates at boundaries.

Subsequently, the graphics portion of the program begins and the user is able to enter either the radial or axial plot mode.

In either mode, nodal coordinates at the specified nodal index are displayed and parameter plots along the entire nodal line may be made using nodal values only, or nodal values with a specified number of interpolated values between nodes. The capability for plotting only a segment of the nodal line also exists and appropriate end points may be specified.

The number of available plot options depends on position and orientation. The following options are always available in both amplitude and phase:

```
1 - Axial velocity
2 - Radial velocity
```

- 3 - Tangential velocity
- 4 - Pressure

In addition, in the axial direction plot mode a fifth option, acoustic flux integrated over that radial plane is available, and is the same regardless of the radial node specified.

Also at any boundary, acoustic admittance may be computed and its real and imaginary parts plotted.

A "no plot" option allows the user to progress to another nodal index station or to change directional mode.

With every plot, scales are set automatically but the user may change them if the resultant plot is not to his liking or to demonstrate a particular facet of the data.

Generally, the following instructions apply to all user input:

- "Y" indicates yes
- "N" indicates no
- "?" displayed on the screen with no prompting directives allows the user time to make a hardcopy of the screen contents. To proceed to the next step, enter "carriage return".

At the conclusion of an interactive session, a directory of all plot frames created during the session are displayed.

If permanent CalComp plots are required, the user may enter the postprocessor program TRN.

Within TRN, no prompting directives are issued and the user is required to know the format of TRN instructions.

For simple use, only three commands are required:

- P - Plot
- S - Skip
- G - Go
- Q - Quit

P and S are followed by a blank space and a number indicating the number of frames the user requires plotted or skipped.

Input commands are separated by blanks, commas or the end of a line.

Thus for example, to plot frames 2, 3, 4 and 7, 8 out of a ten-frame directory, the following instructions would be issued in response to the TRN> prompt:

S 1, P 3, S 2, P 2, G

Then response to the next TRN> prompt:

Q

Procedure FEPLLOT then submits an off-line batch job for creation of the required plots.

Examples of plots created using this process are shown in Section 7.

7 EXAMPLES AND DISCUSSION

MODEL CONFIGURATION

The configuration selected for testing and demonstration of the ADAM system is relatively simple. It consists of a narrow variable area duct with hard walls, approximately three meters long with uniform cylindrical sections at each end tapering gently to a centrally located constriction (see Figure 7.1). The radius of cylindrical sections is 0.15 meter and the area ratio of these sections to the constriction throat is =2.

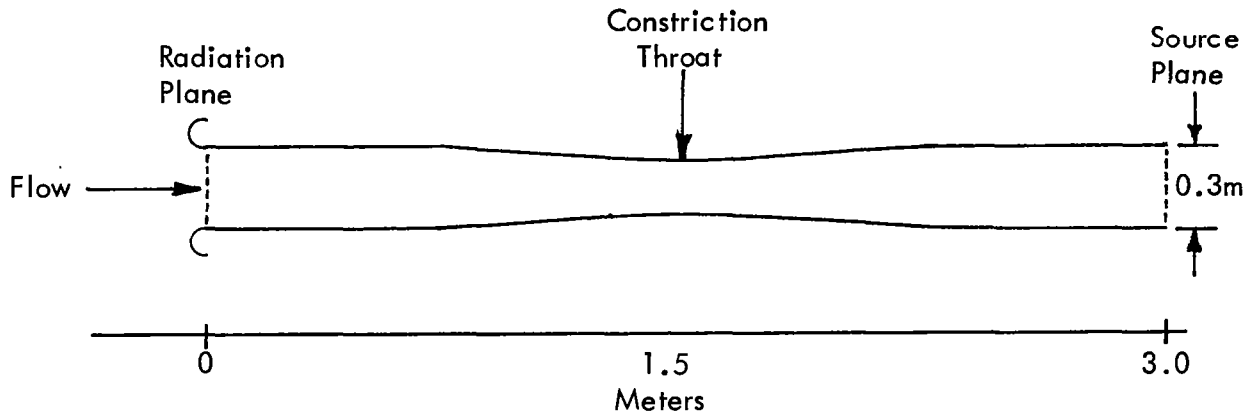


Figure 7.1 Test Case Geometry: Duct With Central Constriction

This configuration has already been analyzed for the "no flow" case by Silcox and Lester³. They found that results from the AFE program agreed well with measured values over a range of modal acoustic source distributions and frequencies.

The purpose of the following examples is to illustrate the format of the ADAM system graphical output and to show that the system produces anticipated results when applied to a simple configuration.

APPROXIMATE ENERGY ANALYSIS

In order to provide an independent assessment of sound propagation characteristics in the duct configuration described above, the following approximate analysis is derived from conservation of energy principles.

Consider the acoustic intensity in a variable area duct with quasi-irrotational flow. Morfeys expression for the intensity vector (see references 24 and 25) is:

$$\vec{N} = p\vec{V} + \bar{p}(\vec{V}_0 \cdot \vec{V})\vec{V} + \frac{1}{\rho c^2} \vec{V}_0 p^2 + \frac{1}{c^2} \vec{V}_0 (\vec{V}_0 \cdot \vec{V}) p \quad (7.1)$$

where \vec{N} and \vec{V} are the acoustic intensity and velocity vectors, respectively, and \vec{V}_0 is the mean velocity vector.

Expanding this expression in terms of its components, taking the time average and assuming mean swirl to be zero, we get the following expression for the time average of the axial acoustic intensity $\langle N_z \rangle$:

$$\begin{aligned} \langle N_z \rangle = \frac{1}{2} \text{Re} \{ & (1+M_z^2) pu^* + M_z M_r pv^* + \frac{1}{\bar{\rho}c} M_z pp^* \\ & + \bar{\rho}c M_z uu^* + \bar{\rho}c M_r uv^* \} \end{aligned} \quad (7.2)$$

where M_r, M_z are the radial and axial Mach numbers, "Re" indicates "real part of" and "*" indicates complex-conjugate.

This is also the expression presently contained in the AFE program and is integrated over a radial plane for computing acoustic flux.

Suppose now that the duct contains a plane wave propagating axially against the mean flow and that minimal reflections are caused by the constriction and duct termination. Since the constriction taper is very gradual, the radial Mach number (M_r) is a second order quantity as is radial acoustic velocity (v).

Under these conditions, acoustic pressure (p) and acoustic axial velocity (u) are in phase and are simply related by the expression:

$$\frac{p}{u} = \bar{\rho}c$$

Equation (7.2) then becomes:

$$\langle N_z \rangle = \frac{1}{2} \{ (1+M_z) p \}^2$$

Acoustic flux (F) is then simply the product of this expression and the cross-sectional area. Since the duct has hard walls and no other energy absorbing mechanisms have been introduced, net flux is conserved with distance down the duct. Setting the flux in the constant area section of the duct equal to the flux at the throat gives an expression for the ratio of the pressures at these two locations:

$$\frac{P_t}{P_c} = \frac{(1 + M_{z_c}) r_c}{(1 + M_{z_t}) r_t} \quad (7.3)$$

where subscript "c" refers to constant area, subscript "t" refers to throat, and r is the radius. Similarly, we find that the expression for acoustic axial velocity ratio (u_t/u_c) is identical to that given for the pressure in equation (7.3).

STC ANALYSES

Two STC analyses with different flow Mach numbers were performed. Input data to the STC program for the higher Mach number case are contained in Appendix 1.

Plots of streamlines, Mach number contours and velocity contours for this case obtained from the flow graphics program are shown in Figures 7.2 through 7.4, respectively*. Similar plots for the high Mach number case are shown in Figures 7.5 through 7.7. Dashed lines (with long dashes) in all flow graphics figures indicate boundary layer thickness while lines constructed of short dashes, on streamline plots only, represent boundary layer displacement thickness.

CORRELATION OF APPROXIMATE ENERGY ANALYSIS WITH RESULTS OF AFE ANALYSES

Using equation (7.3) with the results of the STC analyses, we may determine acoustic pressure ratios between cylindrical duct sections and constriction throat for the two flow cases described above. These pressure ratios, together with that for a zero Mach number, are shown in Table 7.1.

Case Number	M_{z_c}	M_{z_t}	Approx. Energy Analysis	AFE Program Results	
			$\frac{P_t}{P_c}$ (or $\frac{u_t}{u_c}$)	$\frac{P_t}{P_c}$	$\frac{u_t}{u_c}$
1	0	0	1.43	1.45	1.41
2	-.141	-.295	1.74	1.70	1.80
3	-.27	-.69	3.4	2.9	3.6

Table 7.1: Comparison of Acoustic Pressure and Velocity Ratios from Approximate Analysis with AFE Analyses

The Mach numbers shown in Table 7.1 represent average Mach numbers across a radial plane. With regard to these values, it is interesting to note that although the area ratio of constant duct section to constriction throat is equal to 2, the ratios of the Mach numbers only approximate to this value (i.e. 2.1 and 2.6). This is the result of compressibility in the flow program and its effects become more pronounced at higher Mach numbers.

*Figures 7.2 through 7.27 follow the text in Section 7.

Correlation for No Flow

From the preceding approximate analysis and from the results presented in the above table, we may thus expect that a plane wave propagating down the duct in the absence of mean flow would exhibit equal uniform pressure amplitudes in the constant area sections increasing to 1.43 times their magnitude at the throat of the constriction. Also, the axial component of acoustic velocity would be expected to display identical characteristics.

Results from an AFE analysis using linear elements with a mesh consisting of 20 radial elements by 400 axial elements are shown in Figures 7.8 through 7.16. Source pressure distribution is uniform and frequency is 512Hz, well below the cut-on frequency for higher order radial modes.

Figures 7.8 and 7.9 show the axial dependence of acoustic pressure, amplitude and phase, along a line located approximately midway between duct centerline and outer wall.

As expected, pressure in Figure 7.8 is approximately constant in constant area sections of the duct and peaking near the constriction throat with an amplitude close to the value predicted by the approximate analysis (see Table 7.1). The parallel straight phase lines in Figure 7.9 are characteristic of plane wave propagation. Clearly, the approximate analysis is not quite correct in assuming no reflections from duct constriction and termination as shown by the standing wave pattern superimposed on the basic pressure characteristic in Figure 7.8.

Axial dependence of the amplitudes of axial and radial velocity components along the same line is shown in Figures 7.10 and 7.11, respectively. Axial velocity displays a similar trend to pressure (Figure 7.8), while radial velocity is nonzero only in nonuniform sections of the duct. Interestingly, it tends to drop quickly towards zero as the duct walls briefly become parallel at the constriction throat.

Other assumptions of the approximate analysis are verified by the results in Figures 7.12 through 7.18. Acoustic flux integrated over radial cross-sections is shown to be conserved (Figure 7.12), a plane wave evidenced by constant radial pressure profiles is seen to be propagating in uniform sections of the duct (Figures 7.13 and 7.14), and acoustic admittance of the duct outer wall is zero (Figures 7.15 and 7.16).

Correlation With Flow

For the case of sound propagation along the duct in the opposite direction to the mean flow the approximate analysis shows that the relative heights of the pressure, and axial velocity peaks at the duct constriction throat increase with flow velocity (see Table 7.1).

AFE analyses using Hermite elements with first order derivatives only, on a mesh of 11 radial elements by 50 axial elements for the two nonzero flow cases in Table 7.1 were performed using the axial points distribution function in Figure 6.3 with the explicit radial points distribution function and the DATASUB example also shown in section 6. Results are presented in

Figures 7.17 through 7.26.

Figures 7.17 and 7.21 show axial dependence of acoustic pressure amplitude along a line approximately midway between duct centerline and outer wall for the two nonzero axial flow velocities in Table 7.1, respectively. Ratios of throat to uniform section pressures are seen to increase with flow velocity to a peak agreeing closely with values predicted by the approximate model (see Table 7.1). Axial velocity components along the same line increase in a similar manner as shown in Figures 7.19 and 7.23.

Comparing Figures 7.9, 7.18, and 7.22, axial dependence of acoustic pressure phase shows the expected effect of increased mean flow velocity by an increased rate of change with distance. This axial rate of change of phase with distance corresponds to the propagation constant (k) in a one-dimensional model. Based on a one-dimensional model, it would be expected that k would have the following dependence on Mach number (M):

$$k = \frac{k_0}{1-M}$$

where k_0 is the axial propagation constant for zero flow.

The effect of this nonlinear dependence on Mach number is seen by the magnified effect of the constriction in the higher Mach number case (Figure 7.22) compared to the lower Mach number case (Figure 7.18).

Acoustic flux is again conserved in both cases as shown in Figures 7.20 and 7.24.

CHECKERBOARDING

A common phenomenon in Galerkin finite element formulations known as "checkerboarding" (references 26, 27), or "cusping" (reference 21) is sometimes observed in areas where large mean flow gradients are present or where mesh resolution is inadequate. Sometimes the presence of a localized problem may cause an instability which spreads and contaminates the entire solution.

The presence of tolerable levels of contamination is shown in Figures 7.25 through 7.27. These three figures are all parts of the same three AFE solutions discussed earlier. Figure 7.25 represents the axial variation of the axial components of acoustic velocity amplitude along a line close to the wall for case 3. Due to the presence of the boundary layer (where large mean velocity gradients exist), small oscillations are superimposed on the true solution. A magnified example from the same case for the radial velocity component is shown in Figure 7.26. Here the high level of contamination is tolerable due to the small overall magnitude of the radial velocity component compared to the axial component and its negligible contribution to the overall solution.

Even in apparently very stable solutions, some level of checkerboarding is frequently present. Figure 7.27 shows the effects of greatly magnifying the scale on the linear element solution radial plot (Figure 7.13) from the AFE no flow analysis of case 1.

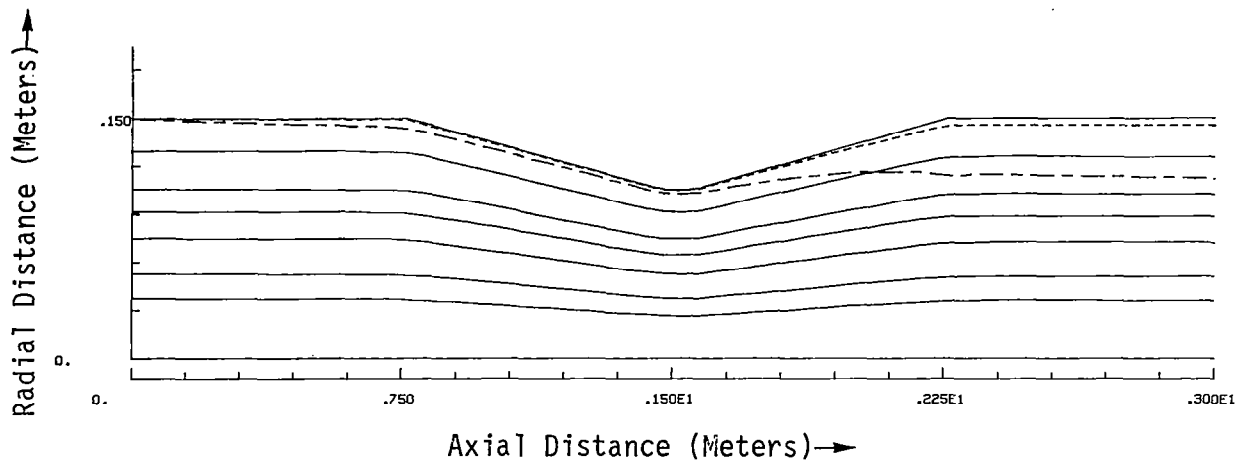


Figure 7.2 Streamlines for Case 2

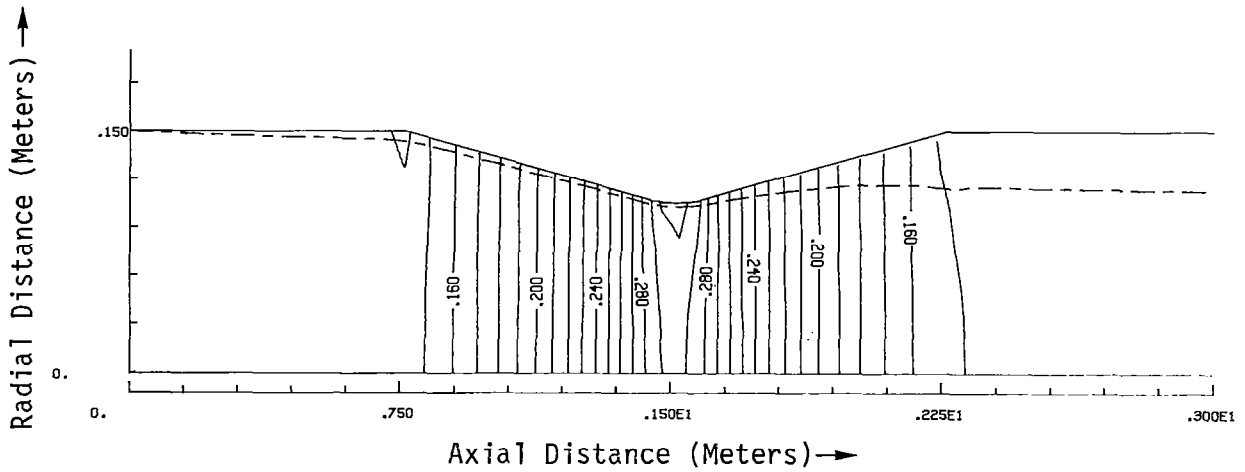


Figure 7.3 Mach Number Contours from .13 to .3 (interval=.01) for Case 2

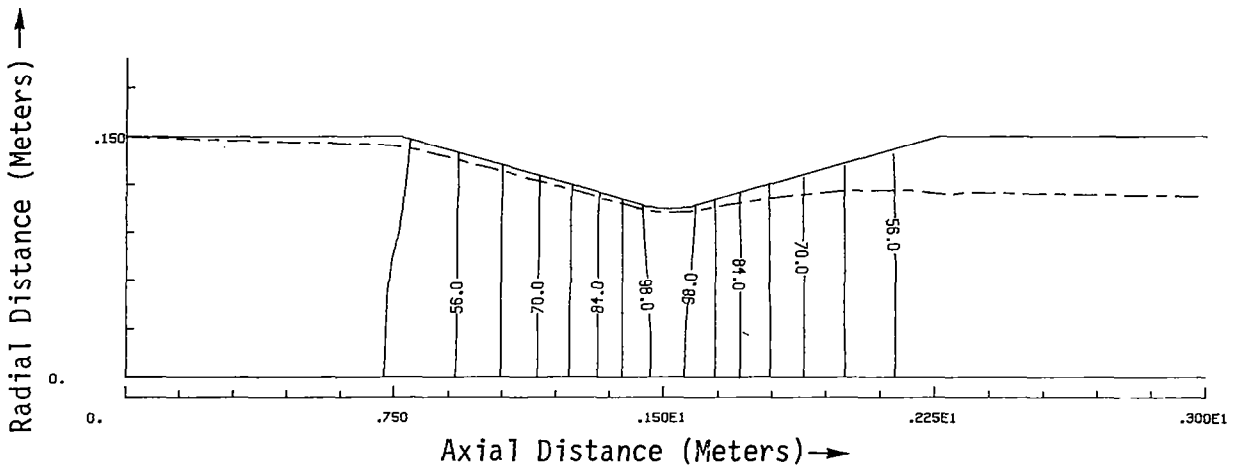


Figure 7.4 Velocity Contours from 42 to 98 (interval=7) for Case 2

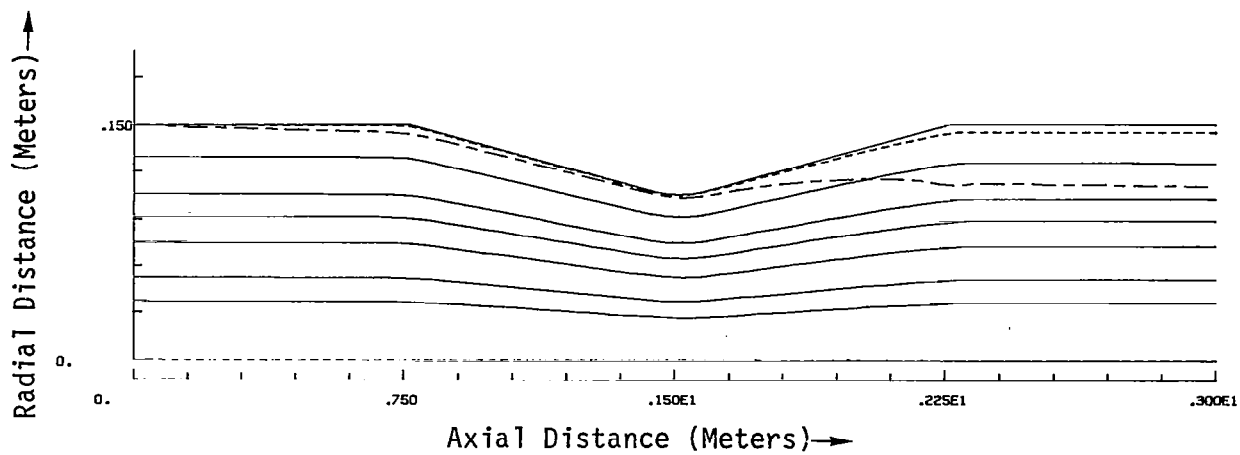


Figure 7.5 Streamlines for Case 3

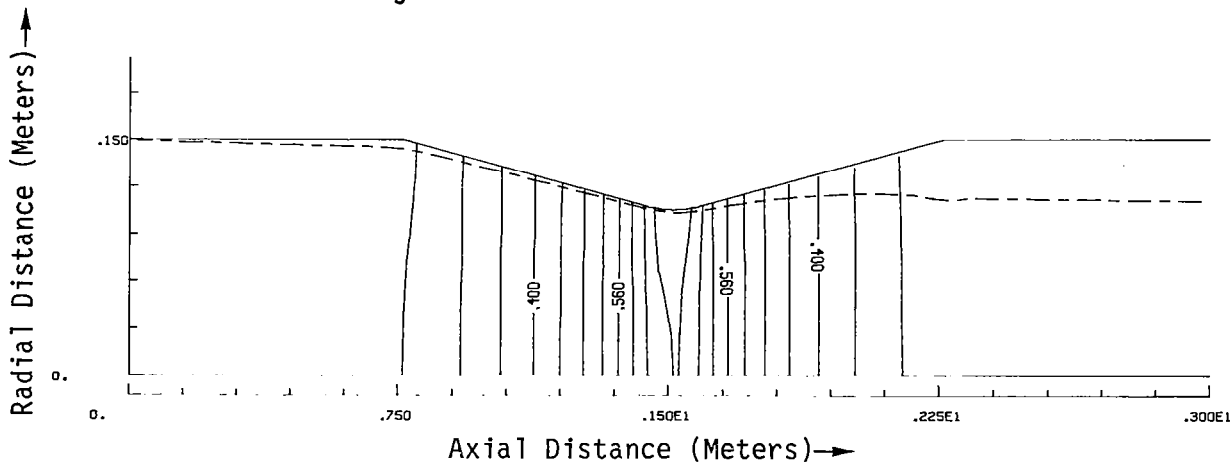


Figure 7.6 Mach Number Contours from .24 to .68 (interval=.04) for Case 3

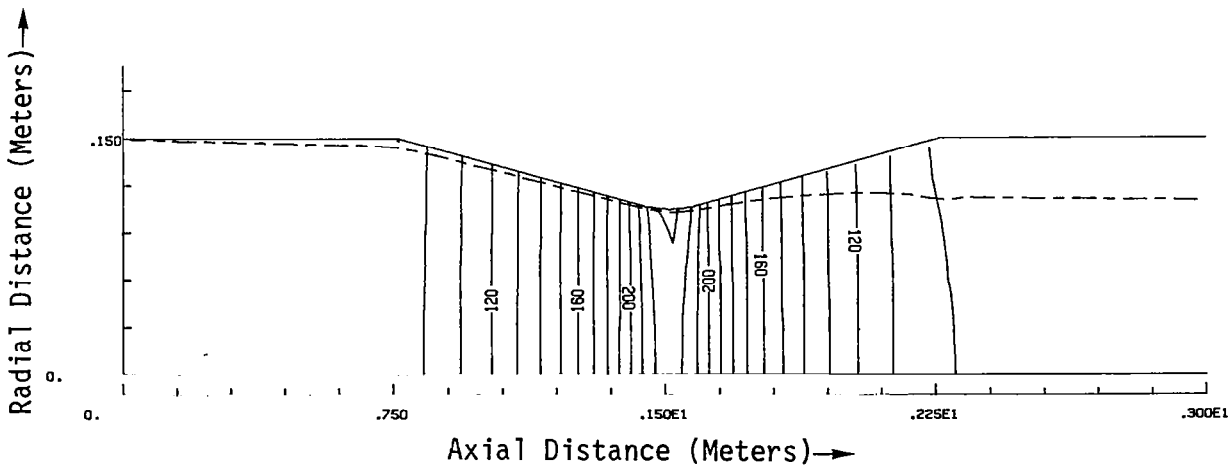


Figure 7.7 Velocity Contours from 80 to 230 (interval=.04) for Case 3

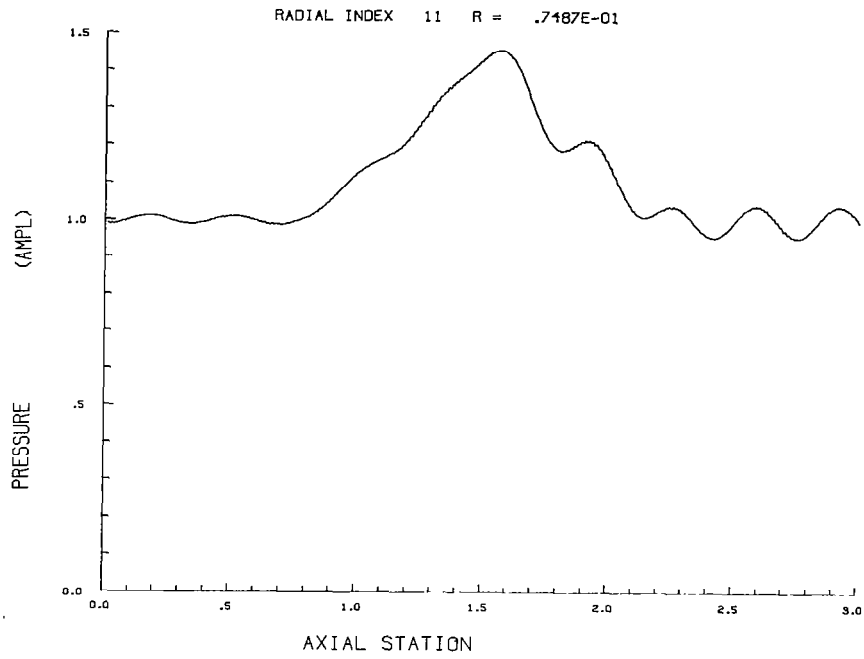


Figure 7.8 Axial Plot of Pressure Amplitude for Case 1 (No Flow)

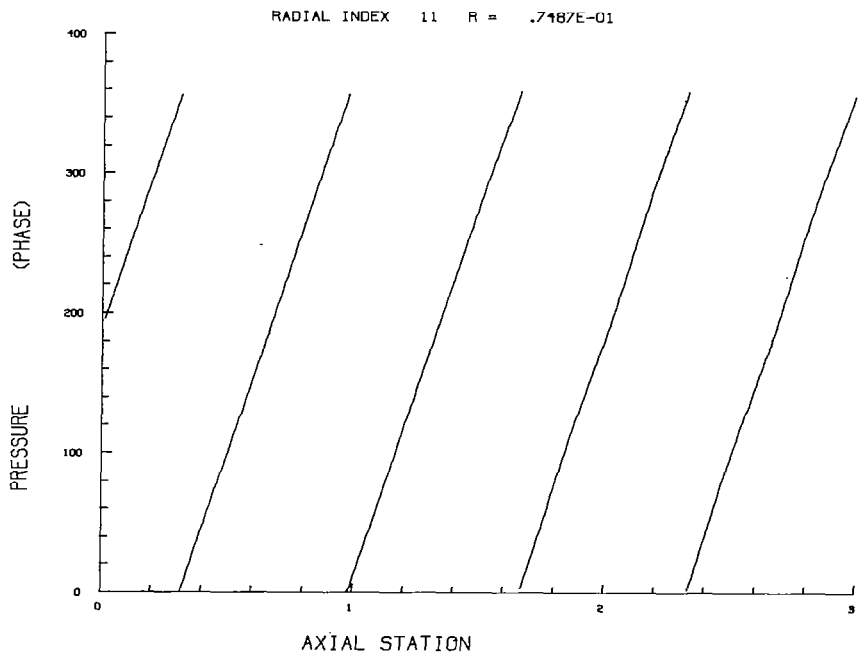


Figure 7.9 Axial Plot of Pressure Phase for Case 1 (No Flow)

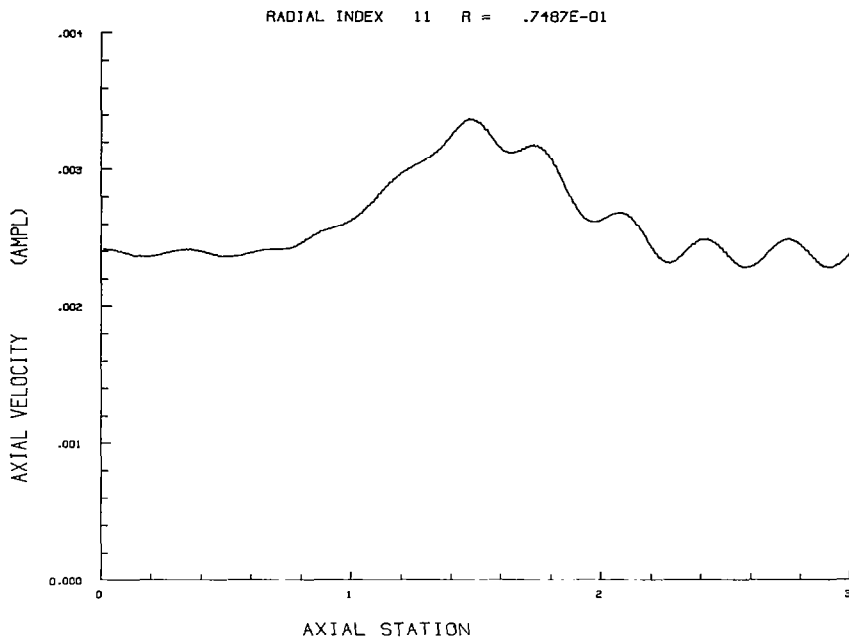


Figure 7.10 Axial Plot of Axial Velocity Amplitude for Case 1 (No Flow)

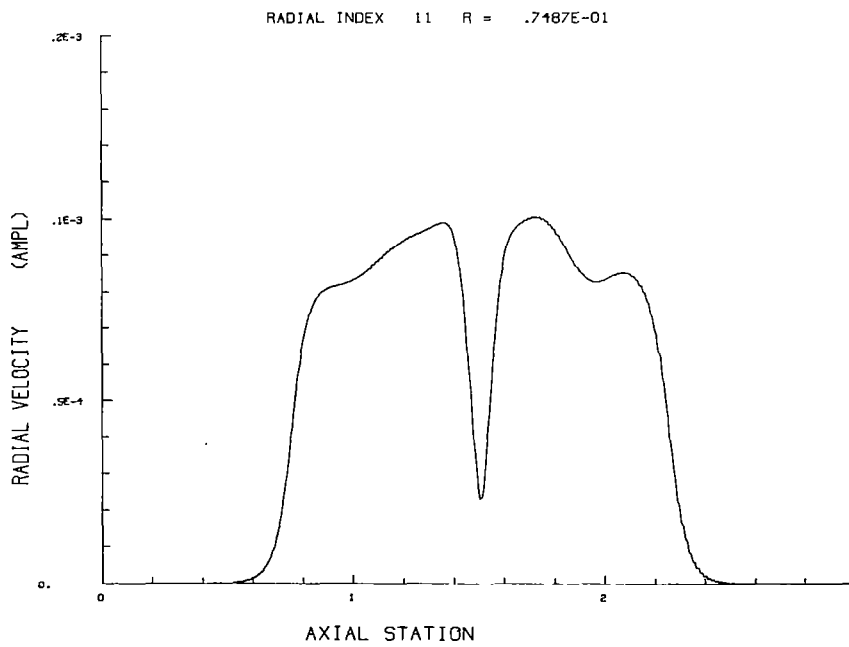


Figure 7.11 Axial Plot of Radial Velocity Amplitude for Case 1 (No Flow)

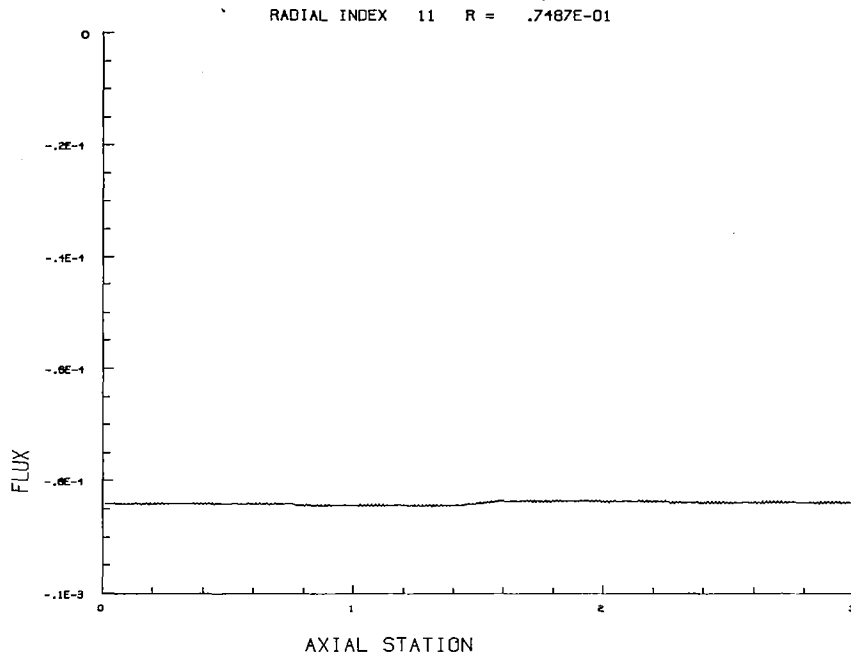


Figure 7.12 Axial Plot of Acoustic Flux Integrated over Successive Radial Planes for Case 1 (No Flow)

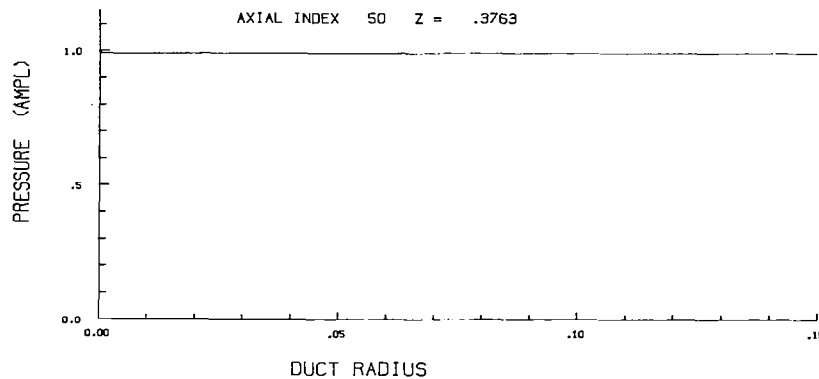


Figure 7.13 Radial Plot of Pressure Amplitude for Case 1 (No Flow), Axial Index 50, $z = .3763\text{m}$

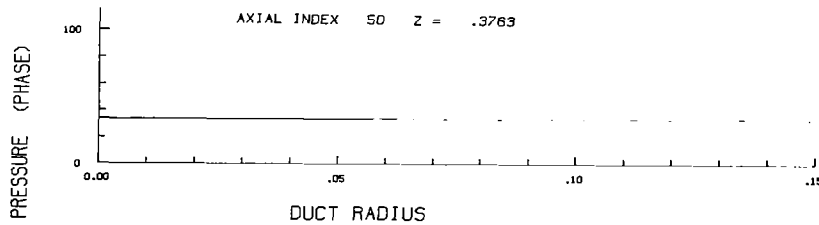


Figure 7.14 Radial Plot of Pressure Phase for Case 1 (No Flow), Axial Index 50, $z = .3763\text{m}$

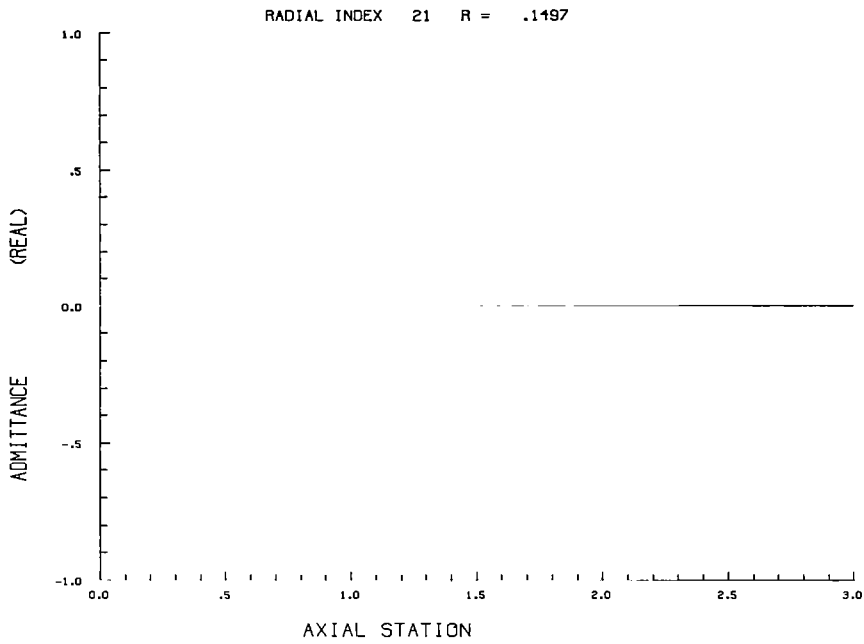


Figure 7.15 Axial Plot of the Real Part of Outer Wall Specific Acoustic Admittance for Case 1 (No Flow)

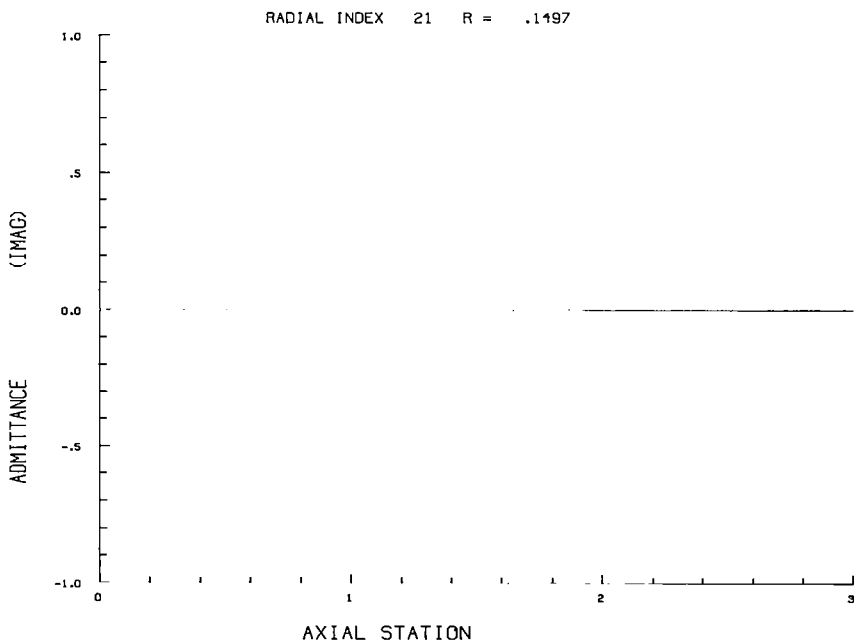


Figure 7.16 Axial Plot of the Imaginary Part of Outer Wall Specific Acoustic Admittance for Case 1 (No Flow)

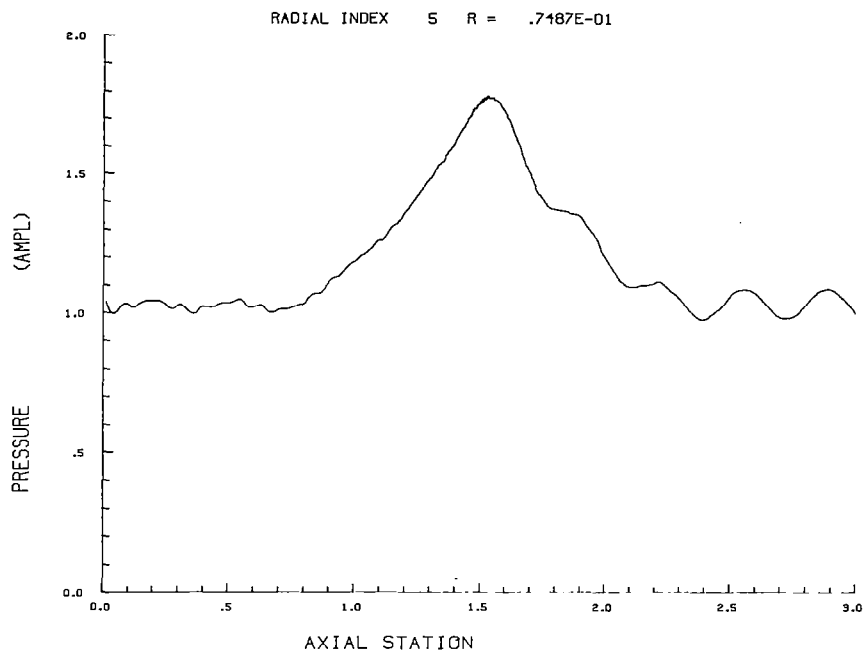


Figure 7.17 Axial Plot of Pressure Amplitude for Case 2 Flow

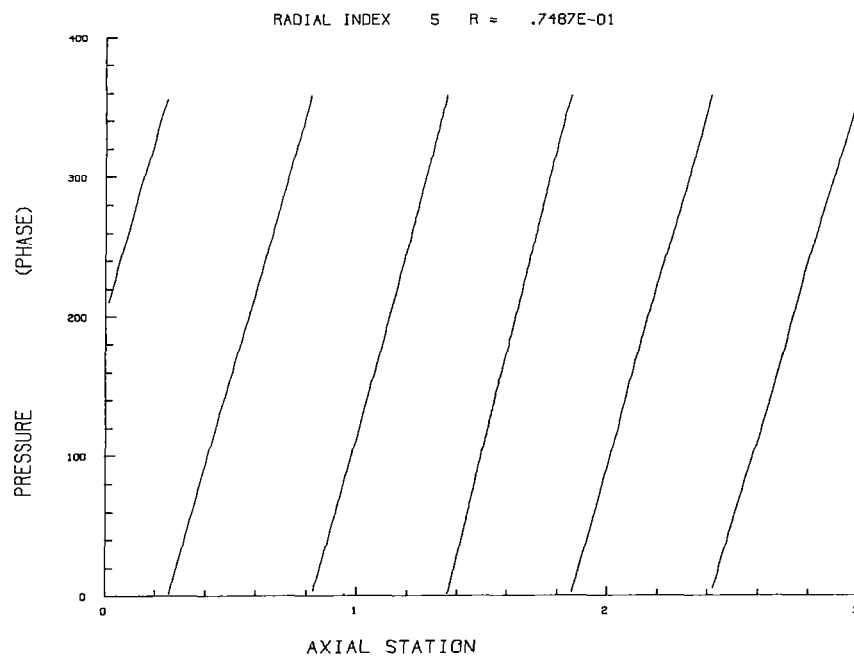


Figure 7.18 Axial Plot of Pressure Phase for Case 2 Flow

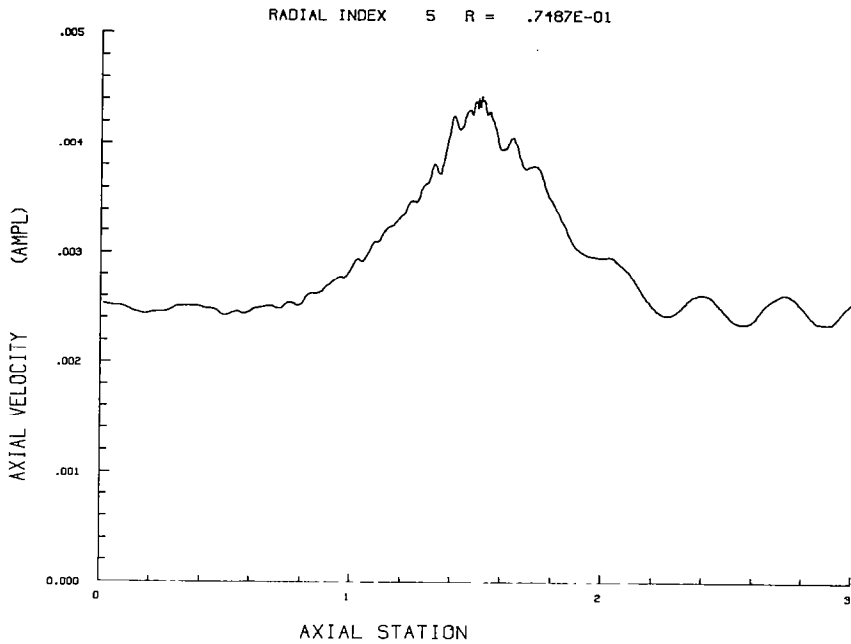


Figure 7.19 Axial Plot of Axial Velocity Amplitude for Case 2 Flow

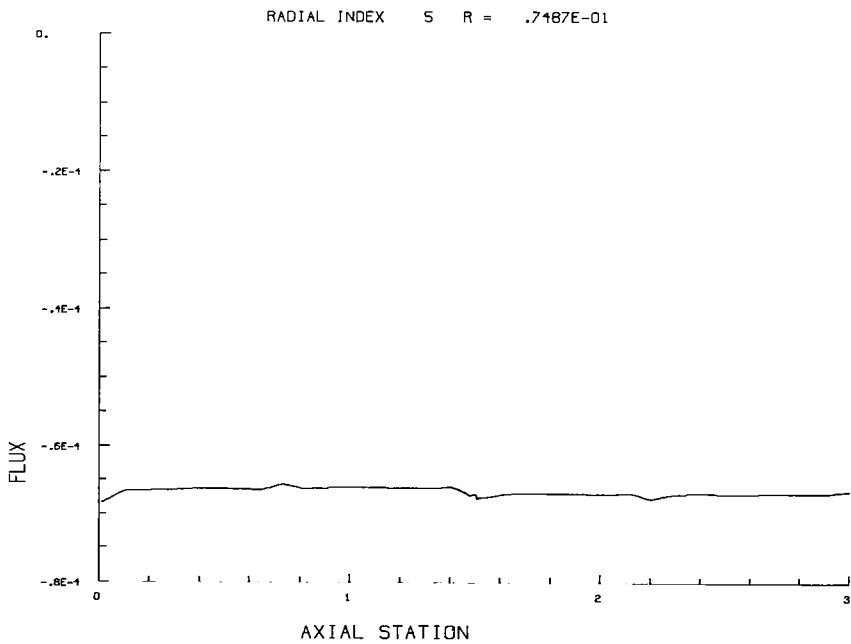


Figure 7.20 Axial Plot of Acoustic Flux Integrated over Successive Radial Planes for Case 2 Flow

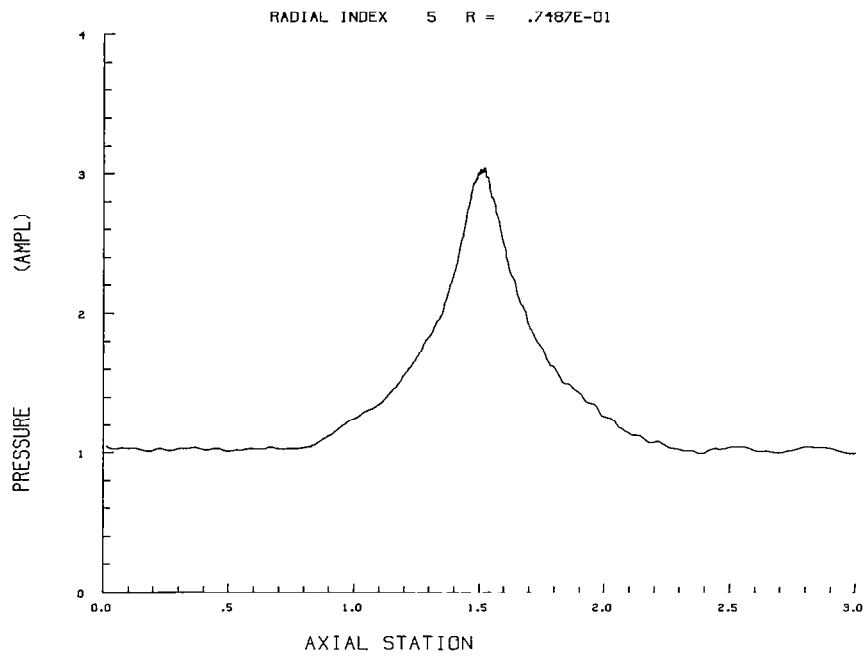


Figure 7.21 Axial Plot of Pressure Amplitude for Case 3 Flow

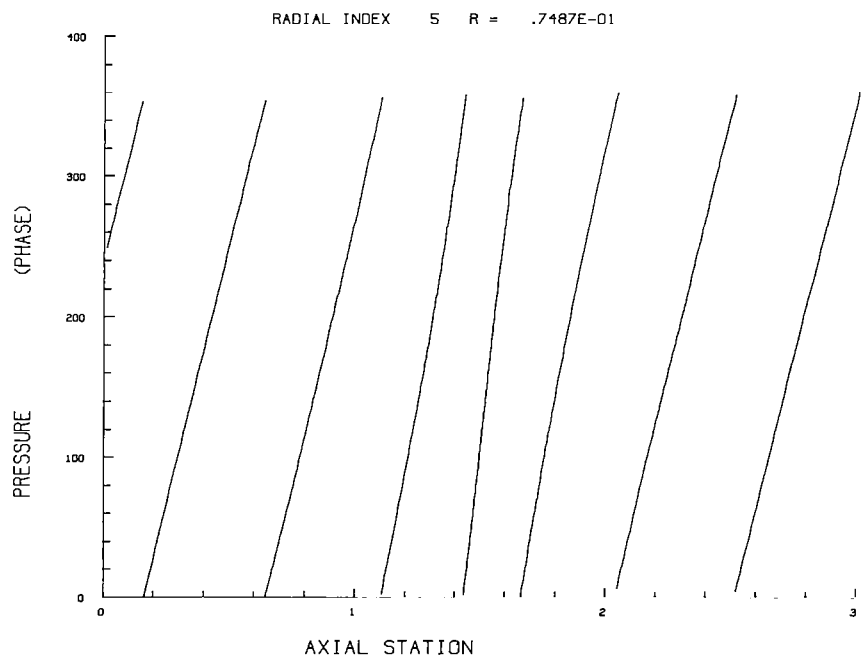


Figure 7.22 Axial Plot of Pressure Phase for Case 3 Flow

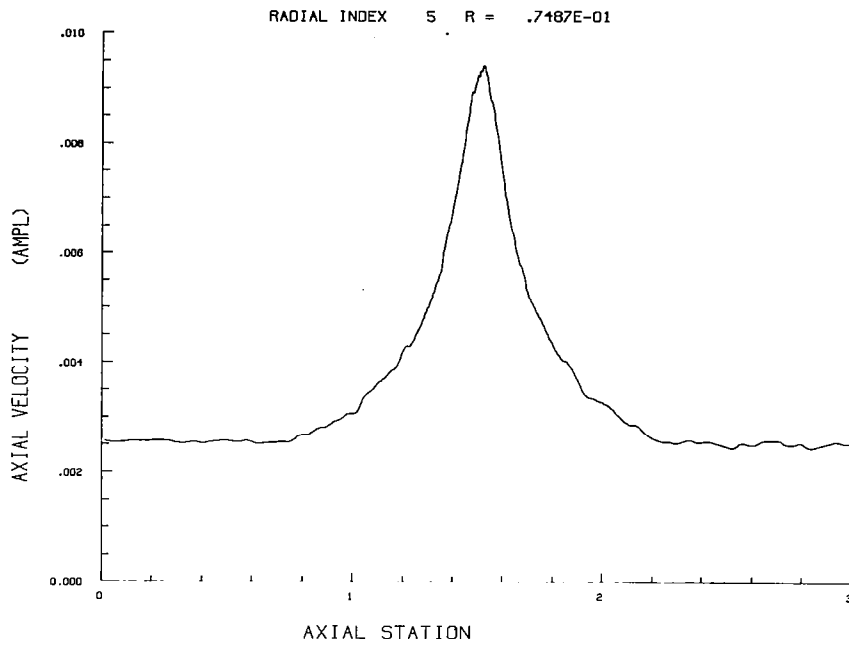


Figure 7.23 Axial Plot of Axial Velocity Amplitude for Case 3 Flow

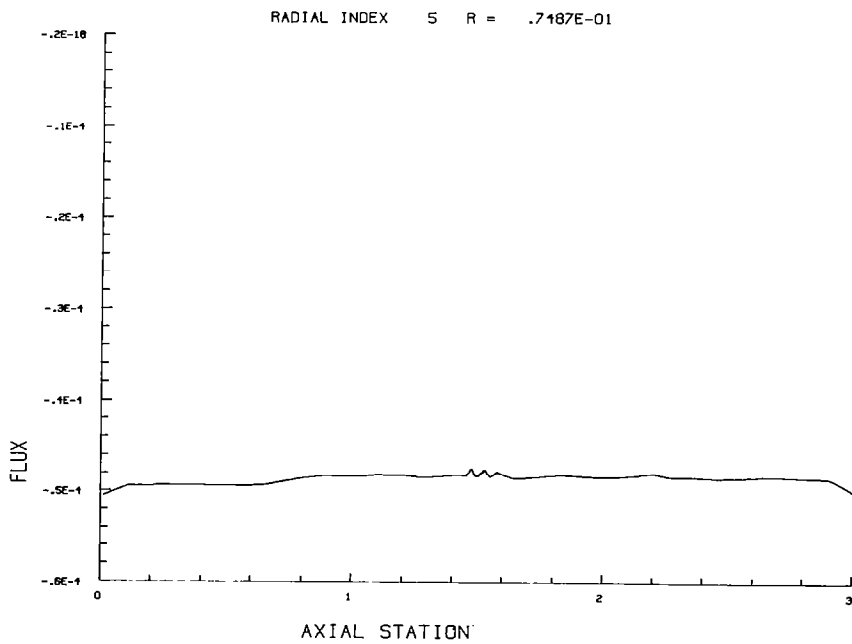


Figure 7.24 Axial Plot of Acoustic Flux Integrated over Successive Radial Planes for Case 3 Flow

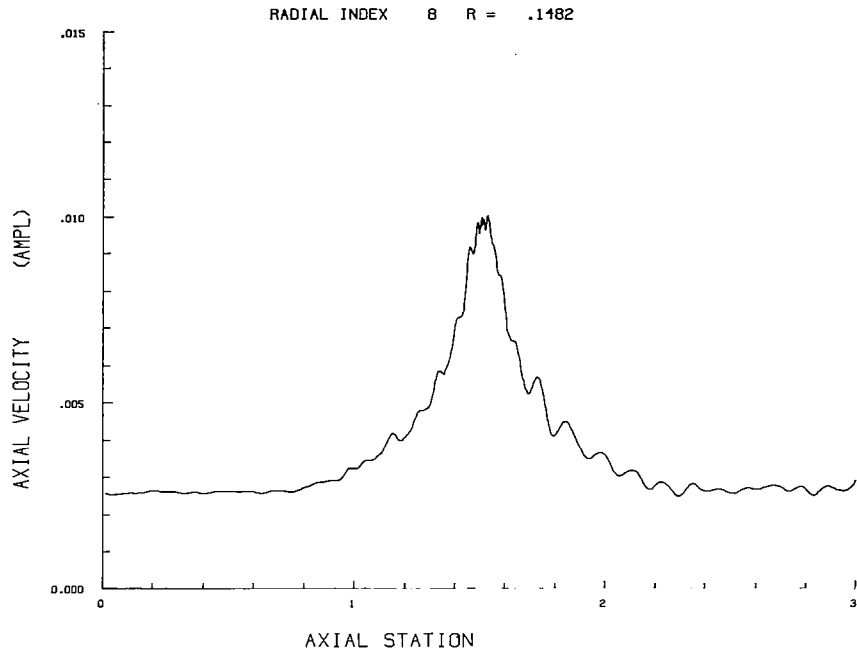


Figure 7.25 Axial Plot of Axial Velocity Amplitude for Case 3 Flow

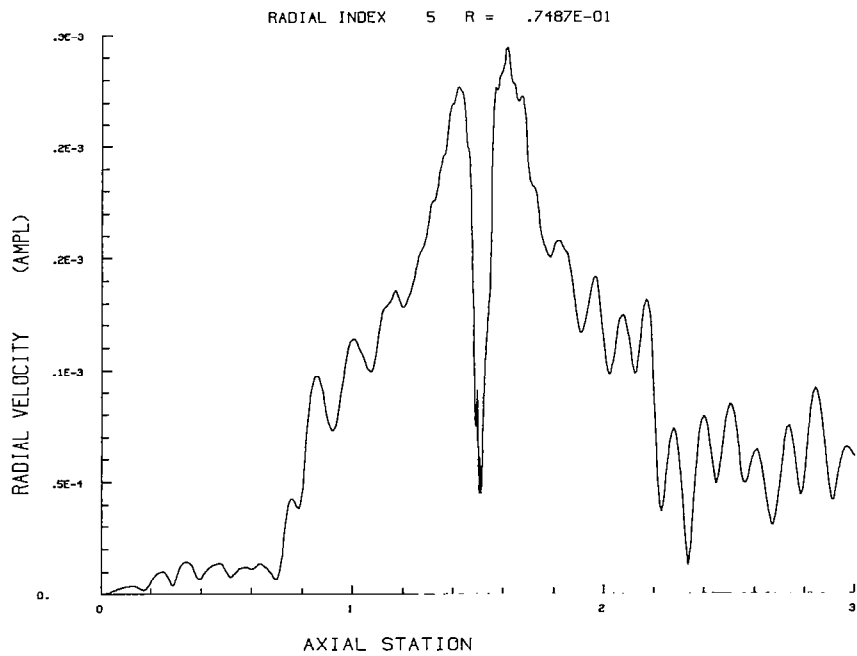


Figure 7.26 Axial Plot of Radial Velocity Amplitude for Case 3 Flow

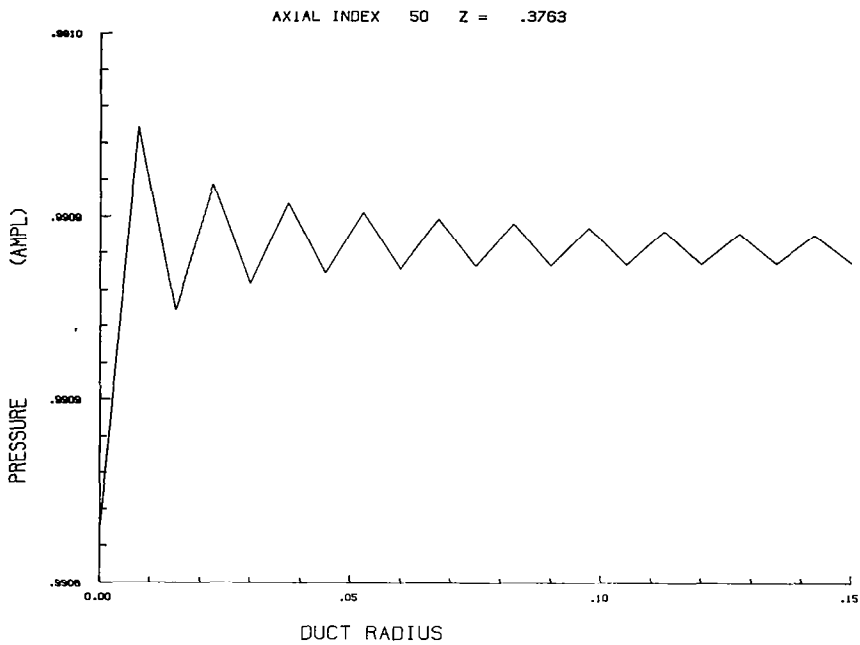


Figure 7.27 Radial Plot of Pressure Amplitude for Case 1 (No Flow)

Note: This plot is identical to Figure 7.13 with the pressure scale greatly enlarged.

8 SUMMARY

This report describes an advanced system for the analysis of sound propagation in axisymmetric (or planar) ducts containing near sonic compressible mean flows.

The system derives its unique capabilities from the integration of a thoroughly tested computer code for derivation of the mean flow with an established finite element code for solution of the acoustic problem.

Also of significance are steps which were taken to make the system "friendly" to the user. These include the addition of powerful interactive graphics for interpretation and analysis of results and the introduction of simplified operating procedures through use of advanced features of CDC-NOS on NASA Langley Research Center's Cyber computers.

The Adam system is considered to represent a significant step forward in facilitating advanced aeroacoustic duct analyses both for research and design.

REFERENCES

1. Parrott, T. L., and Lester, H. C., "Calculated and Measured Performance of a Near Ideal Locally Reacting Duct Liner in Grazing Incidence," Paper presented at AIAA 6th Aeroacoustics Conference, June 1980.
2. Lester, H. C., and Parrott, T. L., "Application of Finite Element Methodology for Computing Grazing Incidence Wave Structure in an Impedance Tube: Comparison with Experiment," Paper presented at AIAA 5th Aeroacoustics Conference, March 1979.
3. Silcox, R. J., and Lester, H. C., "Sound Propagation Through a Variable Area Duct: Experiment and Theory," Paper presented at AIAA 7th Aeroacoustics Conference, October 1981.
4. Baumeister, K. J., "Numerical Techniques in Linear Duct Acoustics - 1980/81 Update," NASA Technical Memorandum 82730 prepared for the 102nd Winter Annual Meeting of the ASME, November 1981.
5. Baumeister, K. J., "Numerical Techniques in Linear Duct Acoustics - A Status Report," Journal of Engineering for Industry, pages 270-281, Vol. 103, August 1981.
6. Baumeister, K. J. "Time Dependent Difference Theory for Noise Propagation in a Two-Dimensional Duct," AIAA Journal, Vol. 18, No. 12, December 1980.
7. Baumeister, K. J., "A Time Dependent Difference Theory for Sound Propagation in Ducts with Flow," Paper presented at 98th Meeting of the Acoustical Society of America, Salt Lake City, Utah, November 1979.
8. Baumeister, K. J., "Time Dependent Difference Theory for Sound Propagation in Axisymmetric Ducts with Plug Flow," Paper 80-1017 presented at AIAA 6th Aeroacoustics Conference, June 1980.
9. Abrahamson, A. L., "A Feasibility Study of a 3-D Finite Element Solution Scheme for Aeroengine Duct Acoustics," Paper presented at the 100th Meeting of the Acoustical Society of America," November 1980.
10. Nayfeh, A. J., Kaiser, J. E., and Shaker, B. S., "A Wave-Envelope Analysis of Sound Propagation in Nonuniform Circular Ducts with Compressible Mean Flows." NASA CR-3109, 1979.
11. Baumeister, K. J., "Finite Difference Theory for Sound Propagation in a Lined Duct with Uniform Flow using the Wave Envelope Concept," NASA TP-1001, August 1977.
12. Baumeister, K. J., "Wave Envelope Analysis of Sound Propagation in Ducts with Variable Axial Impedance," Progress in Aeronautics and Astronautics, Vol. 44, pages 451-474, American Institute of Aeronautics and Astronautics, New York, 1976.

13. Nayfeh, A. H., Shaker, B. S., and Kaiser, J. E., "Transmission of Sound Through Non-Uniform Circular Ducts with Compressible Mean Flow," Paper 79-0622 presented at AIAA 5th Aeroacoustics Conference, Seattle, Washington, March 1979.
14. Abrahamson, A. L., "A Finite Element Algorithm for Sound Propagation in Axisymmetric Ducts Containing Compressible Mean Flow." NASA CR-145209, 1977.
15. Abrahamson, A. L., "A Finite Element Algorithm for Sound Propagation in Axisymmetric Ducts Containing Compressible Mean Flow" Paper presented at AIAA 4th Aeroacoustics Conference, Atlanta, Georgia, October 1977.
16. Abrahamson, A. L., "A Finite Element Analysis of Sound Propagation in Axisymmetric Ducts with Compressible Flow," Paper presented at 9th International Congress on Acoustics, Madrid, Spain, July 1977.
17. Ferguson, D. R., and Keith, J. S., "Modifications to the Streamtube Curvature Program, Vol. 1 - Program Modifications and Users Manual and Vol. 2 - Program Listing," NASA CR-132705 and 132706, 1975.
18. Keith, J. S., Ferguson, D. R., Merkle, C. L., Heck, P. H., and Lahti, D. J., "Analytical Method for Predicting the Pressure Distribution about a Nacelle at Transonic Speeds," NASA CR-2217, 1973.
19. Stratford, B. S., and Beavers, G. S., "The Calculation of the Compressible Turbulent Boundary Layer in an Arbitrary Pressure Gradient - A Correlation of Certain Previous Methods," R. & M. No. 3207, British A.R.C., 1961.
20. Astley, R. J., and Eversman, W., "A Finite Element Method for Transmission of Sound in Non-Uniform Ducts Without Flow: Comparison with the Method of Weighted Residuals," Journal of Sound and Vibration, Vol. 27, No. 3, 1978.
21. Astley, R. J., and Eversman, W., "The Application of Finite Element Techniques to Acoustic Transmission in Lined Ducts with Flow," Paper 79-0660 presented at AIAA 5th Aeroacoustics Conference, Seattle, Washington, March 1979.
22. Astley, R. J., and Eversman, W., "Acoustic Transmission in Non-Uniform Ducts with Mean Flow, Part II: The Finite Element Method," Journal of Sound and Vibration, Vol. 74, No. 1, 1981.
23. Gottlieb, D., Gunzburger, M., and Turkel, E., "On Numerical Boundary Treatment of Hyperbolic Systems for Finite Difference and Finite Element Methods," SIAM Journal of Numerical Analysis, Vol. 19, No. 4, 1982.
24. Morfey, C. L., "Acoustic Energy in Non-Uniform Flows," Journal of Sound and Vibration, Vol. 14, No. 2, 1971.

25. Eversman, W., "Acoustic Power Balance in Lined Ducts," Paper 79-0620 presented at AIAA 5th Aeroacoustics Conference, Seattle, Washington, March 1979.
26. Donea, J., Guiliani, S., Morgan, K., and Quartapelle, L., "The Significance of Chequerboarding in a Galerkin Finite Element Solution of the Navier Stokes Equations," International Journal for Numerical Methods in Engineering, Vol. 17, pages 790-795, 1981.
27. Lee, R. L., Gresho, P. M., and Sani, R. L., "Smoothing Techniques for Certain Primitive Variable Solutions of the Navier Stokes Equations," International Journal for Numerical Methods in Engineering, Vol. 14, pages 1785-1804, 1979.

APPENDIX 1

Sheet 1

Overall Input Data

▼
2
▼
1 STC _____ _____
input tape? output tape?
T or F T or F

Mach number, ambient pressure and temperature, fluid properties
\$A (1.) (1.) (1.) (1.4)
MACH0=_____, TOS=_____, PSO=_____, RG=_____, GAM=_____.

Highlight radius, maximum body radius, body closure tolerance
RHL=_____, RM=_____, TTE=_____,

Axisymmetric or Planar?
T or F

AXI=_____,
spatial grid refinement criteria, see notes
GR(1)=_____, _____, _____, _____, _____, _____, _____,
SGR(1)=_____, _____, _____, _____, _____, _____, _____,
NGR=_____,
GZ(1)=_____, _____, _____, _____, _____, _____, _____,
SGZ(1)=_____, _____, _____, _____, _____, _____, _____,
NGZ=_____,

maximum Mach number increment between grid points
streamwise normal
direction direction
(0.1) (0.1)

VMG1=_____ VMG2=_____

maximum number curvature damping incompressible start
of refinements (1.) (0)

MAXIT=_____ RHOC=_____ NODENS=_____

fluid reference temperature, reference viscosity Sutherland constant, unit
conversion constant
(518.7⁰r) (10⁻⁶lbm/in.sec) (198.6⁰ R)

TREF=_____, MUREF=_____, SCON=_____,

\$

Sheet 3a

Restart Procedure for Merging STC
Solution with Boundary Layer

These data follow Sheet 3 and are simply repeats of Sheet 1 with "input tape" set to "true". To use this procedure, "output tape" must be set to "true" on the original Sheet 1.

column 2 ↓		Input tape? T or F	Output tape T or F
1	STC	<u>T</u>	<u>T</u>
\$A			
\$			
1	STC	<u>T</u>	<u>T</u>
\$A			
\$			
1	STC	<u>T</u>	<u>T</u>
\$A			
\$			

The above example performs three restarts. More may be added as required until it is seen that the solution is fully converged.

Specimen Card Input

NAME=
ADDRESS=
IDENT=CONICAL-CIRCULAR CONSTRICTION A/A*=2.0351
1 STC F T
\$A
MACH0=0.14,TS0=516.665,PS0=14.5,RG=1716.0,
RHL=5.895,RM=5.895,TTE=0.0,
AXI=T,
GR(1)=0.0,5.895,
SGR(1)=0.75,0.75,
NGR=2,
GZ(1)=-53.0,-35.0,-20.0,0.0,20.0,35.0,53.0,
SGZ(1)=3.0,3.0,0.5,0.1,0.5,3.0,3.0,
NGZ=7,
VMG1=50.0,VMG2=75.0,
MAXIT=2,PRPRN=-1.0,
\$
2 BDY CL INT
\$A
UPPER=F,ZRONLY=F,BL=F,
B(1)=-53.0,0.0,0.0,
53.0,0.0,0.0,
\$
2 BDY CNLCIR INT
\$A
UPPER=T,ZRONLY=F,BL=T,
B(1)=-53.0,5.895,0.0,
-29.475, 5.895,0.0,
-29.4687,5.8948, -3.6075,
-3.0203, 4.2271, -3.6075,
-2.9303, 4.2215, -3.5,
-2.5121, 4.1978, -3.0,
-2.0937, 4.1777 -2.5,
-1.6752, 4.1612, -2.0,
-1.2565, 4.1484, -1.5,
-0.8377, 4.1393, -1.0,
-0.4189, 4.1338, -0.5,
0.0, 4.132, 0.0,
0.4189, 4.1338, 0.5,
0.8377, 4.1393, 1.0
1.2565, 4.1484, 1.5
1.6752, 4.1612, 2.0,
2.0937, 4.1777, 2.5
2.5121, 4.1978, 3.0
2,9303, 4.2215, 3.5,
3.0202, 4.2271, 3.6075,
29,4687, 5.8948, 3.6075,
29.475, 5.895,0.0,
53.0,5.895,0.0,
\$

```
3 CHN      INT
$A
RG=1716.0,VARY=T,A0=1.0,
$
1 STC      T      T
$A MAXIT=4, $
1 STC      T      T
$A
MACH0=.295,TS0=509.815,PS0=13.8385,
MAXIT=7,
$
1 STC      T      T
$A MAXIT=7, $
1 STC      T      F
$A MAXIT=8,PRPRN=1.0,$
```


Appendix 1 - Addendum - Additional STC Program Controls

Part A - Optional input which may follow sheet 1

A large number of input quantities that are additional to those described in the main body of this report may be specified. These items are not normally required for execution of the STC program and consist in general of controls for special program options and input data to modify preset or initialized constants or parameters.

Only the following selected few of these optional input parameters are described here (for a full list see reference 17):

Flow Balance and Flow Adjustment Tolerances

		<u>Preset Value</u>
TOLES2	Final solution tolerance on streamline position error (=MAXES2)	.001
TOLINR	Intermediate solution tolerance on MAXES2	.05
NINNER (1)	Number of inner iterations without grid refinement. Specify up to MAXIT Values	16*10
CNVF (1)	Fractional percentage of total point movement to be used at a given refinement level. Specify up to MAXIT Values.	10*1.0
TOLWF	Tolerance on fractional flow adjustment needed to meet trailing edge pressure closure condition.	.001

(A more detailed explanation of the function of these parameters is contained in the following section).

Grid Refinement Parameters

The following items may be used to control the length of orthogonal lines and streamlines as the grid is refined. If set equal to zero, they ensure that all new grid lines will span the entire field.

CRXSL	Control for extending streamlines	.375
CRXOL	Control for extending orthogonal lines across a subsonic region.	.375

Part B - Notes on interpretation of solution history output

This output section describes the progress of the STC iterative solution algorithm. Here, the behavior of MAXES2 relative to LIMES2 indicates con-

vergence by a decreasing absolute value as the solution proceeds. Any erratic behavior in MAXES2 indicates convergence problems.

Sometimes MAXES2 will start to converge and then show instability. By identifying the appropriate NINNER, the solution can be forced to the previous level of grid refinement by rerunning the problem with the NINNER control inserted. Convergence difficulties for this type of problem may sometimes be overcome by establishing a refined grid at a lower Mach number and then slowly raising the Mach number to the desired level using restart cases.

Definitions of parameters listed in the solution history follow:

NREFINE - The number of times the grid has been refined. The maximum number of grid refinements is controlled by input parameter MAXIT.

GRIDPTS - The number of points in the flow field.

INRCTR - The number of inner iterations at the current grid refinement level. These are controlled by built in tolerances on the flow balance, but may be overridden by inputting NINNER(M) where M is the level of grid refinement.

NSSPTS - Number of imbedded supersonic points in the flow field.

NSWEEPS - Number of sweeps through the matrix solution on the current inner iteration.

MAXDS2 - Maximum streamline adjustment actually made during the current inner iteration.

LIMES2 - $TOLINR * (\text{current grid size})$, where TOLINR is an optional input parameter specifying a tolerance on grid development, i.e., grid development in the inner loop continues provided $MAXES2 < LIMES2$ (unless preceded by other conditions).

(r,z) - Field coordinates of point with maximum streamline movement.

The utility of TOLINR is that it permits a looser tolerance on inner iterations while grid development is taking place. Finally, when grid development is satisfactorily achieved, then a final tight tolerance (TOLES2) assumes control, and flow field definition continues until $MAXES2 < TOLES2 * CLEN$ where $CLEN = (\text{Average of SGR's and SGZ's})$.

APPENDIX 2

Format of AFE12 Output File

(Total number of Records = $2N + 4$)

Record 1 - AFE Program Input Data Identifiers

M = Number of elements in radial direction
N = Number of elements in axial direction
NPHPAR = Number of acoustic physical parameters at a node
NNDERIV = Number of nodal derivatives of each parameter
FLOW = "True" if flow data on GE file was used
 = "False" for no flow
FREQ = Acoustic Frequency

Record 2 - STC Program Input Data Identifiers

NAME (6), IDENT (6), MACH0, TSO, PSO, RG,
NAMEBDY (2), UPPER (2), BL (2)

Record 3 - Aerodynamic parameters from STC program interpolated on AFE mesh

AERODAT (M1, N1, 2) = Mach number and flow angle at each node

Record (3+J) - Data for AFE row #J (i.e. nodal rows J and J+1)

(N Records of length $4(M+1) + 16M$)

RZ (2, M1, 2) = Nodal coordinates

Index 3 = 1 : J'th nodal row
 = 2 : (J+1)'th nodal row

Index 2 = 1 to M1 : Radial node number

Index 1 = 1 : R coordinates
 = 2 : Z coordinates

JAC (4, 4, M) = Jacobian matrices for J'th AFE row

Index 3 = 1 to M for elements in radial direction

Indices 1 & 2 : e.g. = $J_{1k} = \text{JAC}(1, k, I)$
 $J_{4k} = \text{JAC}(4, k, I)$

Record (3 + N + J) - Solution vectors for J'th radial nodal rows (and flux).

(N+1) Records of length $NPHPAR * NNDERIV * (M+1) * 2+1$ = real and imaginary parts of solution vectors with flux in last location.

Order of variables is as follows:

$$u, \frac{\partial u}{\partial r}, \frac{\partial u}{\partial z}, \frac{\partial^2 u}{\partial r \partial z}, v, \frac{\partial v}{\partial r}, \frac{\partial v}{\partial z}, \frac{\partial^2 v}{\partial r \partial z}, w, \frac{\partial w}{\partial r}, \frac{\partial w}{\partial z}, \frac{\partial^2 w}{\partial r \partial z}, p, \frac{\partial p}{\partial r}, \frac{\partial p}{\partial z}, \frac{\partial^2 p}{\partial r \partial z}.$$

1. Report No. NASA CR-3668	2. Government Accession No.	3. Recipient's Catalog No.	
4. Title and Subtitle ADAM - AN AXISYMMETRIC DUCT AEROACOUSTIC MODELING SYSTEM		5. Report Date January 1983	6. Performing Organization Code
		8. Performing Organization Report No.	
7. Author(s) A. Louis Abrahamson		10. Work Unit No.	
9. Performing Organization Name and Address COMTEK 123 East Woodland Road Grafton, Virginia 23692		11. Contract or Grant No.	
		13. Type of Report and Period Covered Contractor Report	
12. Sponsoring Agency Name and Address National Aeronautics and Space Administration Washington, D.C. 20546		14. Sponsoring Agency Code 505-31-33-13 L-34073B	
		15. Supplementary Notes Langley Technical Monitor: Harold C. Lester Final Report	
16. Abstract <p>ADAM is an acronym for Axisymmetric Duct Aeroacoustic Modeling and is the name of an interconnected system of computer programs for analysing the propagation and attenuation of sound in aeroengine ducts containing realistic compressible subsonic mean flows. It has been developed primarily for research directed towards the reduction of noise emitted from turbofan aircraft engines and includes as two basic components a streamtube curvature program for determination of the mean flow and a finite element code for solution of the acoustic propagation problem.</p> <p>The system, which has been specifically tailored for ease of use, is presently installed at NASA Langley Research Center on a Control Data Cyber 175 Computer under the NOS Operating System employing a Tektronix terminal for interactive graphics.</p> <p>This report describes the scope and organization of the ADAM System and includes a users guide, examples of input data and results for selected cases.</p>			
17. Key Words (Suggested by Author(s)) Duct Acoustics Sound Propagation Noise Control		18. Distribution Statement Unclassified - Unlimited Subject Category 71	
19. Security Classif. (of this report) Unclassified	20. Security Classif. (of this page) Unclassified	21. No. of Pages 90	22. Price A05